

# Black Hole Chemistry Knows Extra Dimensions

---

**Kyung Kiu Kim,<sup>a,d</sup> Jeongwon Ho,<sup>b,d</sup> Seungjoon Hyun,<sup>c</sup> Taehyeon Song<sup>c</sup>**

<sup>a</sup>College of General Education, Kookmin University, Seoul 02707, Korea

<sup>b</sup>Center for Quantum Spacetime, Sogang University, Seoul 04107, Korea

<sup>c</sup>Department of Physics, Yonsei University, Seoul 03722, Korea

<sup>d</sup>Korea Research Network for Theoretical Physics, Seoul 02707, Korea

*E-mail:* [sjhyun@yonsei.ac.kr](mailto:sjhyun@yonsei.ac.kr), [kimkyungkiu@kookmin.ac.kr](mailto:kimkyungkiu@kookmin.ac.kr),  
[freejwho@gmail.com](mailto:freejwho@gmail.com), [sthing@yonsei.ac.kr](mailto:sthing@yonsei.ac.kr)

**ABSTRACT:** In this note, we study an extra dimension effect on the black hole chemistry in the 8-dimensional Einstein-Yang-Mills-Maxwell theory. The base spacetime contains 4-dimensional compact manifolds and an instanton on top of those. We demonstrate how the extra dimensions affect the phase transition and viable black hole sizes in the 4-dimensional Einstein frame through the black hole chemistry. We focus on asymptotically anti-de Sitter spacetimes for the effective 4-dimensional model obtained by a dimensional reduction. The extra-dimension size determines thermodynamic pressure, and the thermodynamic volume is roughly the horizon size of black holes. Thus, the extra dimension and black hole sizes are related as a conjugate pair of thermodynamic variables. In addition, we discuss the zeroth-order phase transition of the 4-dimensional Kerr-AdS black hole.

**KEYWORDS:** Black thermodynamics, Black hole chemistry, Yang-Mills instanton

---

## Contents

<b>1</b>	<b>Introduction</b>	<b>1</b>
<b>2</b>	<b>4-dimensional Reduced Action in the Einstein Frame</b>	<b>3</b>
2.1	Reduced action for $S^4$	3
2.2	$CP^2$ as extra dimensions	7
2.3	$S^2 \times S^2$ as extra dimensions	8
<b>3</b>	<b>Thermodynamic Volume and Phase Diagram with Extra Dimensions</b>	<b>10</b>
3.1	Schwarzschild black hole	10
3.2	Dyonic black hole with $q = B$	12
3.3	Kerr-AdS black hole	18
3.4	Black hole merging and fission with large extra dimensions	23
<b>4</b>	<b>Conclusion and Discussion</b>	<b>24</b>
<b>A</b>	<b>D=4 Euclidean Kerr-AdS Black Hole</b>	<b>25</b>

---

## 1 Introduction

Black hole chemistry is the extended thermodynamics by identifying the cosmological constant with a bulk pressure [1–6]. Even though this identification seems natural from the bulk point of view, one puzzling aspect may arise because the cosmological constant is a theory parameter that cannot be varied. Nevertheless, black hole chemistry provides a new perspective to demonstrate the Hawking-Page transition [7] as a liquid-solid phase transition [8]. In the context of AdS/CFT, this phenomenon is known as the confinement-deconfinement phase transition in quark-gluon plasma [9]. Therefore, finding the physical meaning of the variation is desirable in explicit gravity systems. In some cases, the ill-defined variation is overcome by introducing a dynamically generated cosmological constant in preceding works [10–12]. The present paper provides another simple model to realize the black hole chemistry with extra dimensions accompanied by an instanton configuration.

This idea of thermodynamic pressure has been widely applied to various systems based on the aforementioned theoretical works. In this new approach, it is discovered that the mass of black holes is no longer the internal energy but the enthalpy [1] and that the Reissner-Nordström (RN)-AdS black hole has a critical point and the Small/Large black hole phase transition, which corresponds to the liquid-gas transition in the Van der Waals fluid [5]. Also, the resultant phase diagrams for various black holes have rich structures showing the reentrant phase transition [13, 14] and the novel triple points [15–17]. See [18] for a review. In addition, this black hole chemistry is applied to numerous interesting

topics such as heat engines, non-standard critical points, superfluid transitions, molecular microstate structures, and so on. See, *e.g.*, [19–22]. The AdS background is also extended to accelerating backgrounds [23–25], flat spacetime [26], de Sitter spacetime [27–29], and soliton backgrounds [30, 31].

Even though varying the cosmological constant can be realized dynamically in gravity theories, a holographic interpretation of black hole chemistry is not easy. The cosmological constant  $\Lambda$  in a holographic model based on the AdS/CFT correspondence [32] is associated with the gauge group rank  $N$  of dual field theory and the Newton constant. Thus, changing  $\Lambda$  could come from changing the Newton constant or  $N$ . So far, three ways have been proposed for variation of  $\Lambda$ . One is the consideration of the  $1/N$  correction with higher derivative terms in the large  $N$  limit [33, 34]. Another is extending the system with a conjugate chemical potential to the central charge [35]<sup>1</sup>. The other way is changing the volume of the corresponding CFT [37]. These directions are studied actively, and it would lead to an extension of AdS/CFT correspondence. See [38] for a recent review.

The present work focuses on the 8-dimensional Einstein-Yang-Mills-Maxwell system with a cosmological constant. The spacetime is decomposed into Lorentzian and Euclidean 4 dimensions. The 4-dimensional Euclidean space is regarded as a compact-regular manifold and as extra dimensions on which Yang-Mills (YM) instantons sit. It is known that there are three kinds of manifolds appropriate to our case:  $S^4$ ,  $CP^2$  and  $S^2 \times S^2$ . This instanton structure on extra dimensions is used for generating a stable Minkowski spacetime [39] or studying cosmological evolution with dynamical compactification [40–43]. On the other hand, the present work will be devoted to studying the black hole configurations in the context of black hole chemistry.

Our interest is restricted by the following ansatz for the full metric:

$$ds^2 = g_{\mu\nu}(x)dx^\mu dx^\nu + L^2 e^{2f(x)} h_{ab}(y)dy^a dy^b, \quad (1.1)$$

where  $L$  is a length scale related to a given cosmological constant in the 8-dimensional theory, and  $\mu, \nu$  and  $a, b$  stand for the Lorentzian and Euclidean 4-dimensional spacetimes, respectively; furthermore, we focus on the warping factor  $f(x)$  supposed to be a constant. This warping factor governs the size of the extra dimensions, which is determined by the instanton number in our analysis. This instanton number, equivalently, the size of the extra dimensions changes the effective cosmological constant in the 4-dimensional reduced action. Thus, taking this cosmological constant as a thermodynamic variable is legitimate.

Our main results are the phase diagrams regarding the extra-dimension size accompanied by the temperature and the disallowed size data of the black holes. We study three cases: 4-dimensional Schwarzschild, Dyonic, and Kerr-AdS black holes. The Schwarzschild black hole undergoes the Hawking-Page transition. The transition temperature from the black hole to thermal AdS decreases as the extra-dimension size increases. In addition, the lower bound of the black hole size increases as the extra dimension size increases. Thus, the large extra dimension doesn't allow most small black holes in the context of the black hole chemistry.

---

<sup>1</sup>An earlier proposal for a chemical potential conjugate to the number of M2-branes is in [36].

Also, we consider two kinds of black holes for the Small/Large black hole transition. One is the dyonic black hole with equal electric and magnetic charges, and the other is the Kerr-AdS black hole. The equality of both charges of the former case is required by taking a constant warping factor  $e^{2f(x)}$  in (1.1). The phase diagrams of the dyonic and rotating black holes tell us that the transition temperature decreases as the extra-dimension size increases. Also, the disallowed size range of black holes broadens as the extra-dimension size increases. This implies that a larger extra-dimension size than the critical size results in a size gap between small and large black holes. Therefore, size data for existing black holes in this fictitious AdS world can be used to infer the size of the extra dimensions. Notably, our example shows how the black hole chemistry is related to a physical consequence. It would be interesting to consider this phenomenon in de Sitter spacetime using results of the extended works [27–29].

As a by-product, we found that even the 4-dimensional Kerr-AdS black hole undergoes a zeroth-order phase transition in the canonical ensemble. This is from the cowboy’s lasso shape of the Gibbs free energy. The zeroth-order phase transition shows up commonly in the black hole chemistry. Various cases including higher dimensional ones of rotating black holes [14, 15, 44, 44–47, 49, 50] and a black hole of dilaton system [51, 52] have already been reported. However, to our knowledge, we couldn’t find any work discussing the zeroth-order phase transition in the black hole chemistry of the 4-dimensional Kerr-AdS black hole. Therefore, our fully numerical result is the first analysis of this black hole.

This paper is organized as follows. Section 2 is devoted to obtaining the 4-dimensional reduced action with the  $\mathbb{S}^4$  extra dimensions in the Einstein frame. Also, this section finds the stable vacua and discusses how to deal with the other compact manifolds,  $\mathbb{CP}^2$  and  $\mathbb{S}^2 \times \mathbb{S}^2$ . In section 3, we reproduce the phase diagrams for the AdS-Schwartzschild, AdS-Dyonic, and Kerr-AdS black holes and construct the phase diagrams regarding the extra-dimension size. In addition to these phase diagrams, we show each case’s disallowed size range of the black holes. Then, section 4 concludes our paper and provides future directions.

## 2 4-dimensional Reduced Action in the Einstein Frame

This section is devoted to deriving a 4-dimensional reduced action from the 8-dimensional action. We will consider  $\mathbb{S}^4$ ,  $\mathbb{CP}^2$ , and  $\mathbb{S}^2 \times \mathbb{S}^2$  as the compact manifold. In [42, 43], the authors show that the only compact Einstein manifolds that are consistent with the instanton configuration and our ansatz are  $\mathbb{S}^4$ ,  $\mathbb{CP}^2$ , and  $\mathbb{S}^2 \times \mathbb{S}^2$ . Here, two  $\mathbb{S}^2$ ’s in  $\mathbb{S}^2 \times \mathbb{S}^2$  has the same radius. In addition,  $\mathbb{S}^2 \times \mathbb{S}^2$  can be extended to non-Einstein manifolds with different radii.

### 2.1 Reduced action for $\mathbb{S}^4$

Let us start with an Einstein-Yang-Mills-Maxwell system with a cosmological constant. The gauge group is chosen as  $SU(2) \times U(1)$ , then the action is given by

$$S_{tot} = S_{grav} + S_{gauge} , \tag{2.1}$$

where

$$\begin{aligned}
S_{grav} &= \frac{1}{16\pi\mathbf{G}_{(8)}} \int d^8x \sqrt{-G} (R - 2\Lambda) \\
S_{gauge} &= \int d^8x \sqrt{-G} \left( \frac{1}{4g_{\text{YM}}^2} \text{Tr} F_{MN} F^{MN} - \frac{1}{4e^2} \mathcal{F}_{MN} \mathcal{F}^{MN} \right). \tag{2.2}
\end{aligned}$$

Here,  $e$  is the coupling of the  $U(1)$  gauge field and  $g_{\text{YM}}$  is that of the  $SU(2)$  gauge field. All the fields associated with  $SU(2)$  are matrix-valued. For instance,  $F_{MN} \equiv F_{MN}^i \tau^i$ , where  $\tau^i$  is the generator of  $SU(2)$  group. The normalization of the generators is taken as  $\text{Tr} \tau^i \tau^j = -\delta^{ij}$ . The equations of motion are given by

$$\begin{aligned}
D_M F^{MN} &= 0, \quad \nabla_M \mathcal{F}^{MN} = 0, \\
R_{MN} - \frac{1}{2} (R - 2\Lambda) G_{MN} &= 8\pi\mathbf{G}_{(8)} \left( T_{MN}^{U(1)} + T_{MN}^{SU(2)} \right), \tag{2.3}
\end{aligned}$$

where  $D_M$  denotes the covariant derivative of the  $SU(2)$  gauge field. The energy-momentum tensors are given as follows:

$$\begin{aligned}
T_{MN}^{U(1)} &= \frac{1}{e^2} \left( \mathcal{F}_M^P \mathcal{F}_{NP} - \frac{1}{4} G_{MN} \mathcal{F}_{PQ} \mathcal{F}^{PQ} \right) \\
T_{MN}^{SU(2)} &= \frac{1}{g_{\text{YM}}^2} \left( \frac{1}{4} G_{MN} \text{Tr} F_{PQ} F^{PQ} - \text{Tr} F_M^P F_{NP} \right) \tag{2.4}
\end{aligned}$$

We continue our study with the following ansatz to find the stable size of extra dimensions:

$$ds^2 = g_{\mu\nu}(x) dx^\mu dx^\nu + L^2 e^{2f(x)} h_{ab}(y) dy^a dy^b \tag{2.5}$$

$$A = A_a(y) dy^a, \quad \mathcal{A} = \mathcal{A}_\mu(x) dx^\mu \tag{2.6}$$

where  $h_{ab}$  is the metric of  $\mathbb{S}^4$  and  $L$  is the length scale of  $\Lambda$ . Thus, we represent the cosmological constant in terms of this scale as

$$\Lambda = \frac{\mathbf{s}}{L^2}, \tag{2.7}$$

where  $\mathbf{s}$  is the sign of  $\Lambda$ , which has a value 1,  $-1$  or 0. In the case of  $\mathbf{s} = 0$ ,  $L$  denotes the length scale related to the physical size of extra dimensions. The nonabelian gauge field  $A$  is taken as an (anti) instanton solution on  $\mathbb{S}^4$ , so  $F$  is (anti) self-dual.

Using the above metric and gauge field configurations, the equations of motions are decomposed as follows:

$$\begin{aligned}
R_{\mu\nu}^{(g)} - \frac{1}{2} R^{(g)} g_{\mu\nu} &= - \left( 4 \nabla^{(g)2} f + 10 \nabla^{(g)} f \cdot \nabla^{(g)} f - \frac{1}{2L^2} e^{-2f} R^{(h)} \right) g_{\mu\nu} \\
&+ 4 \left( \nabla_\mu^{(g)} \nabla_\nu^{(g)} f + \partial_\mu f \partial_\nu f \right) - \frac{8\pi\mathbf{G}_{(8)}}{g_{\text{YM}}^2 L^4} e^{-4f} \rho_n g_{\mu\nu} \\
&- \frac{\mathbf{s}}{L^2} g_{\mu\nu} + \frac{8\pi\mathbf{G}_{(8)}}{e^2} \left( \mathcal{F}_\mu^\lambda \mathcal{F}_{\nu\lambda} - \frac{1}{4} \mathcal{F}_{\lambda\sigma} \mathcal{F}^{\lambda\sigma} g_{\mu\nu} \right)
\end{aligned}$$

$$\begin{aligned}
R_{ab}^{(h)} - \frac{1}{2}R^{(h)}h_{ab} &= 3L^2e^{2f} \left( \frac{1}{6}R^{(g)} - \nabla^{(g)2}f - 2\nabla^{(g)}f \cdot \nabla^{(g)}f \right) h_{ab} \\
&\quad - \mathbf{s}e^{2f}h_{ab} - \frac{8\pi\mathbf{G}_{(8)}L^2}{4e^2}\mathcal{F}_{\mu\nu}\mathcal{F}^{\mu\nu}e^{2f}h_{ab} \\
\nabla_{\mu}^{(g)} \left( e^{4f}\mathcal{F}^{\mu\nu} \right) &= 0,
\end{aligned} \tag{2.8}$$

where all the indices are raised by  $g^{\mu\nu}$  and  $h^{ab}$ , and  $\rho_n = -\frac{1}{4}h^{ac}h^{bd}\text{Tr}F_{ab}F_{cd}$ . In the  $\mathbb{S}^4$  case, the field strength-square is given by  $\rho_n = \frac{H^2}{48}(R^{(h)})^2 = \frac{|n|}{48}(R^{(h)})^2$  for both instanton and anti-instanton, where  $n$  is a winding number of the instanton configuration. This parameter is based on the  $n$ -winding extension of the one-instanton studied in [53]. In addition, we use the following parameters and a curvature choice:

$$\mathcal{R} \equiv R^{(g)}, \quad R^{(h)} = 1, \quad \kappa_4^2 = \frac{8\pi\mathbf{G}_{(8)}}{\mathcal{V}L^4} = 8\pi\mathbf{G}_4, \quad \ell_e^2 \equiv \frac{4\pi\mathbf{G}_{(8)}}{e^2}, \quad \ell_H^2 = \frac{\pi\mathbf{G}_{(8)}|n|}{3g_{\text{YM}}^2}. \tag{2.9}$$

Here,  $\ell_H^2$  is quantized. However, we assume that the ratio of Newton constant to the Yang-Mills coupling is small, which is reasonable due to the weak gravity conjecture [55]. So, we will regard  $\ell_H$  as a continuous parameter.

Together with the above ansatz (2.5-2.6) and the action (2.2), we can integrate out the extra dimension part of the action and obtain the reduced action as follows:

$$\begin{aligned}
S_{tot} &= \frac{\mathcal{V}L^4}{16\pi\mathbf{G}_{(8)}} \int d^4x \sqrt{-g} e^{4f} \left( \mathcal{R} + \frac{1}{L^2}e^{-2f}R^{(h)} + 12\nabla_{\mu}f\nabla^{\mu}f - \frac{2\mathbf{s}}{L^2} \right) \\
&\quad + \mathcal{V}L^4 \int d^4x \sqrt{-g} e^{4f} \left( \frac{1}{4g_{\text{YM}}^2L^4}e^{-4f}\text{Tr}F_{ab}F^{ab} - \frac{1}{4e^2}\mathcal{F}_{\mu\nu}\mathcal{F}^{\mu\nu} \right) \\
&= \frac{1}{2\kappa_4^2} \int d^4x \sqrt{-g} \left\{ e^{4f} \left( \mathcal{R} + 12\nabla_{\mu}f\nabla^{\mu}f - \ell_e^2\mathcal{F}_{\mu\nu}\mathcal{F}^{\mu\nu} \right) \right. \\
&\quad \left. - \frac{2\mathbf{s}}{L^2}e^{4f} + \frac{1}{L^2}e^{2f} - \frac{\ell_H^2}{L^4} \right\},
\end{aligned} \tag{2.10}$$

where  $\mathcal{V} = 3 \cdot 2^7\pi^2$  based on  $R^{(h)} = 1^2$ . The Einstein equation, the Maxwell equation, and the equation of motion of the scalar field  $f$  from this reduced action coincide with the 8-dimensional equations (2.8). Furthermore, one may write down the action (2.10) in the Einstein frame by performing a Weyl transformation  $g_{\mu\nu} = e^{-4f}\tilde{g}_{\mu\nu}$ . The transformed action is

$$\mathcal{I} = \frac{1}{2\kappa_4^2} \int d^4x \sqrt{-\tilde{g}} \left( \tilde{\mathcal{R}} - \ell_e^2e^{4f}\tilde{\mathcal{F}}_{\mu\nu}\tilde{\mathcal{F}}^{\mu\nu} - 12\tilde{\nabla}_{\mu}f\tilde{\nabla}^{\mu}f - V(\mathcal{X}) \right), \tag{2.11}$$

where the potential is given by

$$V(\mathcal{X}) = \frac{2\mathbf{s}}{L^2}e^{-4f} - \frac{1}{L^2}e^{-6f} + \frac{\ell_H^2}{L^4}e^{-8f} = \frac{2\mathbf{s}}{L^2}\frac{1}{\mathcal{X}^2} - \frac{1}{L^2}\frac{1}{\mathcal{X}^3} + \frac{\ell_H^2}{L^4}\frac{1}{\mathcal{X}^4}. \tag{2.12}$$

The tilde “ $\sim$ ” denotes the fields associated with the Einstein frame metric  $\tilde{g}_{\mu\nu}$ . The field  $\mathcal{X}$  is defined as  $\mathcal{X} = e^{2f}$ , so it describes the size of the extra dimensions.

<sup>2</sup>The physical volume of the extra dimension is written by  $\mathcal{V}_{\text{phy}} \equiv \mathcal{V}L^4\mathcal{X}_s^2$ . This is valid even with  $\mathbf{s} = 0$ .

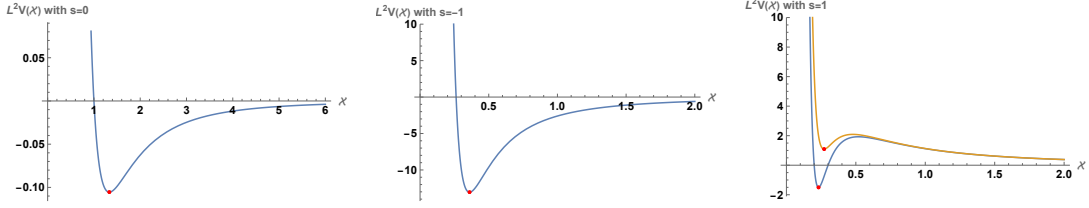


**Figure 1.** Typical shapes of the potential: The red dots denote the stable vacua for the constant warping factor  $e^{2f}$ .

The potential (2.12) determines the stable vacua of this system. Let us see the shapes of the potential for various cases. For  $\mathbf{s} = 0$  and  $-1$  cases, only one extremum exists, corresponding to an AdS vacuum. One can find the typical potentials in Figure 1. On the other hand, the  $\mathbf{s} = 1$  case has two extrema. However, one of them is not stable. As shown in Figure 1, the larger extremum is an unstable vacuum in terms of  $\mathcal{X}$ . Therefore, the smaller extremum is a relevant vacuum as a classical solution. This can be a de Sitter or an anti-de Sitter vacuum depending on the parameter  $\ell_H^2$ . This is reminiscent of the anti-D3 brane uplift in [56]; the origin of the lift to the de Sitter vacua is different, though. We summarize the stable vacua in Table 1.

**Table 1. Stable vacua for the reduced action (2.11)**

$\mathbf{s}$	$\mathcal{X}_s = e^{2f}$	$V(\mathcal{X}_s) = 2\tilde{\Lambda}_{\text{eff}}$	Sign of $V$
+1	$\frac{3}{8} \left( 1 - \sqrt{1 - \frac{64}{9} \frac{\ell_H^2}{L^2}} \right)$ for $\left( \frac{\ell_H}{L} \right) < \frac{3}{8}$	$\frac{2^8}{3^3 L^2 \left( 1 - \sqrt{1 - \frac{64}{9} \left( \frac{\ell_H}{L} \right)^2} \right)^3} \left( 1 - \frac{16}{3} \frac{\left( \frac{\ell_H}{L} \right)^2}{\left( 1 - \sqrt{1 - \frac{64}{9} \left( \frac{\ell_H}{L} \right)^2} \right)} \right)$	$V > 0 \left( \frac{1}{2\sqrt{2}} < \frac{\ell_H}{L} < \frac{3}{8} \right)$ $V < 0 \left( \frac{\ell_H}{L} < \frac{1}{2\sqrt{2}} \right)$
0	$\frac{4}{3} \frac{\ell_H^2}{L^2}$	$-\frac{3^3}{2^8 L^2} \left( \frac{L}{\ell_H} \right)^6$	$V < 0$
-1	$\frac{3}{8} \left( \sqrt{\frac{64\ell_H^2}{9L^2} + 1} - 1 \right)$	$-\frac{2^8}{3^3 L^2} \frac{\frac{16}{3} \left( \frac{\ell_H}{L} \right)^2 + \left( 1 - \sqrt{\frac{64}{9} \left( \frac{\ell_H}{L} \right)^2 + 1} \right)}{\left( 1 - \sqrt{\frac{64}{9} \left( \frac{\ell_H}{L} \right)^2 + 1} \right)^4}$	$V < 0$

Here, one can notice a transition between the de Sitter and anti-de Sitter spacetimes in the case with a positive  $\Lambda(\mathbf{s} = 1)$ . The larger extra-dimension region allows dS spacetimes, while smaller extra dimensions require AdS spacetimes. The transition size of the extra dimensions is  $\mathcal{X} = 1/4$ . This transition is governed by the parameter  $\ell_H^2$  or the instanton number  $n$ .

Our paper will focus on the constant  $\mathcal{X}$  case. Then, the reduced action can be written

as

$$\mathcal{I} = \frac{1}{2\kappa_4^2} \int d^4x \sqrt{-\tilde{g}} \left( \tilde{\mathcal{R}} - \ell_e^2 \mathcal{X}_s^2 \tilde{\mathcal{F}}_{\mu\nu} \tilde{\mathcal{F}}^{\mu\nu} - V(\mathcal{X}_s) \right), \quad (2.13)$$

where  $\mathcal{X}_s$  is a stable size of the extra dimensions. In this constant  $\mathcal{X}$  configuration, expected geometries are dS vacuum, AdS vacuum, and their charged and rotating black holes. These are the main ingredients of the present work.

However, this action is not a consistently truncated one. The equations of motion of the original action (2.11) for the field  $\mathcal{X}$  do not allow a nontrivial function of  $\tilde{\mathcal{F}}_{\mu\nu} \tilde{\mathcal{F}}^{\mu\nu}$ . The only possible configuration is the trivial case. Therefore, the constant  $\mathcal{X}$  configuration demands one more constraint

$$\tilde{\mathcal{F}}^{\mu\nu} \tilde{\mathcal{F}}_{\mu\nu} = 0. \quad (2.14)$$

It seems to be hard to satisfy this constraint for charged black holes. The only possible way to fulfill this condition in four dimensions is to have the same electric and magnetic charges. We will see this case explicitly later, together with the corresponding thermodynamics. In the following subsections, we describe how to deal with  $\mathbb{CP}^2$  or  $\mathbb{S}^2 \times \mathbb{S}^2$  as an extra compact space.

## 2.2 $\mathbb{CP}^2$ as extra dimensions

Let us consider  $\mathbb{CP}^2$  for the extra dimensions. In this case,  $h_{ab}$  in metric ansatz (2.5) can be substituted as

$$h_{ab} dy^a dy^b = \frac{1}{u} (r^2 \sigma_1^2 + r^2 \sigma_2^2) + \frac{1}{u^2} (r^2 \sigma_3^2 + dr^2) = e^a \otimes e^a \quad (2.15)$$

with

$$u(r) = 1 + \frac{\lambda r^2}{6}, \quad (2.16)$$

where  $\lambda$  is a constant representing the size of  $\mathbb{CP}^2$ , and  $r^2 = \sum_{a=1}^4 y_a y_a$ .  $y_a$ 's are coordinates of  $\mathbb{R}^4$ . In addition, the  $\sigma_i$ 's are the left-invariant one-forms on the group manifold of  $SU(2) \cong \mathbb{S}^3$  ( $i = 1, 2, 3$ ). We set  $\lambda = \frac{1}{4}$ , so that  $\mathbb{CP}^2$  has the unit Ricci scalar as in the  $\mathbb{S}^4$  case. The vierbeins can be written as

$$\begin{aligned} e^1 &= \frac{1}{r\sqrt{u(r)}} (-y_4 dy_1 - y_3 dy_2 + y_2 dy_3 + y_1 dy_4) \\ e^2 &= \frac{1}{r\sqrt{u(r)}} (y_3 dy_1 - y_4 dy_2 - y_1 dy_3 + y_2 dy_4) \\ e^3 &= \frac{1}{ru(r)} (-y_2 dy_1 + y_1 dy_2 - y_4 dy_3 + y_3 dy_4) \\ e^4 &= \frac{1}{ru(r)} (y_1 dy_1 + y_2 dy_2 + y_3 dy_3 + y_4 dy_4). \end{aligned} \quad (2.17)$$

Then, we may choose the self-dual  $SU(2)$  gauge field configuration given by

$$A = A^3 \tau^3, \quad A^3 = -\frac{2}{\sqrt{6}} \frac{H}{16} r e^3, \quad (2.18)$$



and the field strength becomes

$$F = F^3 \tau^3, \quad F^3 = \frac{2}{\sqrt{6}} \frac{H}{8} (e^1 \wedge e^2 + e^3 \wedge e^4). \quad (2.19)$$

Hence,  $\text{Tr} F_{ab} F^{ab} = -\frac{H^2}{24}$ . One can perform the dimensional reduction under this self-dual configuration. Then, the reduced action of the  $\mathbb{CP}^2$ -compactification is the same as (2.11) with  $\ell_H^2 = \frac{\pi \mathbf{G}_{(8)} H^2}{6g_{\text{YM}}^2}$ .

### 2.3 $\mathbb{S}^2 \times \mathbb{S}^2$ as extra dimensions

The other nonsingular compact manifold consistent with our ansatz, (2.5) and (2.6), is  $\mathbb{S}^2 \times \mathbb{S}^2$ . Let us choose four angle coordinates as  $(\theta_1, \phi_1, \theta_2, \phi_2)$ , and the radius of each sphere are given by  $\varrho_1$  and  $\varrho_2$ . The metric takes the following form:

$$ds_{\mathbb{S}^2 \times \mathbb{S}^2}^2 = \varrho_1^2 (d\theta_1^2 + \sin^2 \theta_1 d\phi_1^2) + \varrho_2^2 (d\theta_2^2 + \sin^2 \theta_2 d\phi_2^2). \quad (2.20)$$

A natural gauge configuration is given by

$$A = A^3 \tau^3, \quad A^3 = -\frac{H_1}{2} \cos \theta_1 d\phi_1 - \frac{H_2}{2} \cos \theta_2 d\phi_2, \quad (2.21)$$

and the field strength becomes

$$F = F^3 \tau^3, \quad F^3 = \frac{H_1}{2} \sin \theta_1 d\theta_1 \wedge d\phi_1 + \frac{H_2}{2} \sin \theta_2 d\theta_2 \wedge d\phi_2. \quad (2.22)$$

This gauge field satisfies the equation of motion but is not (anti) self-dual unless  $\frac{H_1}{H_2} = \pm (\frac{\varrho_1}{\varrho_2})^2$ .

To see the structure of the equations of motion in a more general ground, we promote the Lorentzian  $(3+1)$  dimensions to the  $(d+1)$  dimensions. The equation of motion from our original action (2.1) can be decomposed into the  $(d+1)$ -dimensional Lorentzian spacetime and two  $\mathbb{S}^2$ 's as follows:

$$\mathcal{R}_{\mu\nu} - \frac{1}{2} g_{\mu\nu} \left( \mathcal{R} + R_{(4)} - 2\Lambda + \frac{4\pi \mathbf{G}_{(D)}}{g_{\text{YM}}^2} \text{Tr} F_{ab} F^{ab} \right) = 8\pi \mathbf{G}_{(D)} T_{\mu\nu}^{U(1)}, \quad (2.23)$$

$$R_{ab}^{(1)} - \frac{1}{2} h_{ab}^{(1)} \left( \mathcal{R} + R_{(4)} - 2\Lambda - \frac{4\pi \mathbf{G}_{(D)}}{e^2} \mathcal{F}^2 \right) = 8\pi \mathbf{G}_{(D)} T_{ab}^{SU(2)}, \quad (2.24)$$

$$R_{cd}^{(2)} - \frac{1}{2} h_{cd}^{(2)} \left( \mathcal{R} + R_{(4)} - 2\Lambda - \frac{4\pi \mathbf{G}_{(D)}}{e^2} \mathcal{F}^2 \right) = 8\pi \mathbf{G}_{(D)} T_{cd}^{SU(2)}, \quad (2.25)$$

where the  $R_{ab}^{(\alpha)}$  ( $\alpha = 1, 2$ ) is the Ricci tensor of  $\alpha$ -th 2-sphere, and the  $h_{ab}^{(\alpha)}$  is metric on that. Each sphere is an Einstein manifold, but their product is not Einstein unless  $\varrho_1 = \varrho_2$ .  $T_{ab}^{SU(2)}$  is proportional to each  $\mathbb{S}^2$  metric for each  $\mathbb{S}^2$  components. Using  $R_{ab}^{(\alpha)} = \frac{1}{2} h_{ab}^{(\alpha)} R^{(\alpha)}$ , (2.24) and (2.25) can be written as a non-self-dual condition for fluxes and the  $(d+1)$ -dimensional curvature as follows:

$$\left( \frac{1}{\varrho_1^2} - \frac{1}{\varrho_2^2} \right) = \frac{2\pi \mathbf{G}_{(D)}}{g_{\text{YM}}^2} \left( \frac{H_1^2}{\varrho_1^4} - \frac{H_2^2}{\varrho_2^4} \right), \quad (2.26)$$

$$\mathcal{R} = \frac{4\pi\mathbf{G}_{(D)}\mathcal{F}^2}{e^2} + 2\Lambda - \left(\frac{1}{\varrho_1^2} + \frac{1}{\varrho_2^2}\right). \quad (2.27)$$

Now, we consider the trace part of (2.23) given by

$$\begin{aligned} \mathcal{R} = & -\left(\frac{d+1}{d-1}\right) \left[2\left(\frac{1}{\varrho_1^2} + \frac{1}{\varrho_2^2}\right) - 2\Lambda - \frac{2\pi\mathbf{G}_{(D)}}{g_{\text{YM}}^2} \left(\frac{H_1^2}{\varrho_1^4} + \frac{H_2^2}{\varrho_2^4}\right)\right] \\ & + \frac{4\pi\mathbf{G}_{(D)}}{e^2} \left(\frac{3-d}{1-d}\right) \mathcal{F}^2. \end{aligned} \quad (2.28)$$

To make this equation consistent with (2.27), we find the  $(d+1)$ -dimensional curvature and  $\mathcal{F}^2$  as follows:

$$\begin{aligned} \mathcal{R} = & 4\Lambda - \frac{1}{2}(d+5) \left(\frac{1}{\varrho_2^2} + \frac{1}{\varrho_1^2}\right) + \frac{(1+d)\pi\mathbf{G}_{(D)}}{g_{\text{YM}}^2} \left(\frac{H_1^2}{\varrho_1^4} + \frac{H_2^2}{\varrho_2^4}\right), \\ \mathcal{F}^2 = & \frac{e^2\Lambda}{2\pi\mathbf{G}_{(D)}} - \frac{(d+3)e^2}{8\pi\mathbf{G}_{(D)}} \left(\frac{1}{\varrho_2^2} + \frac{1}{\varrho_1^2}\right) + \frac{(d+1)e^2}{4g_{\text{YM}}^2} \left(\frac{H_1^2}{\varrho_1^4} + \frac{H_2^2}{\varrho_2^4}\right). \end{aligned} \quad (2.29)$$

In a generic case,  $\mathcal{F}^2$  is a nontrivial function of coordinates. Thus we restrict our consideration to  $\mathcal{F}^2 = 0$  case, where the curvature becomes:

$$\mathcal{R} = \frac{2(d+1)}{d+3} \left[ \Lambda - \frac{\pi\mathbf{G}_{(D)}}{g_{\text{YM}}^2} \left(\frac{H_1^2}{\varrho_1^4} + \frac{H_2^2}{\varrho_2^4}\right) \right]. \quad (2.30)$$

The above result shows that a simple extension of the non-Einstein  $\mathbb{S}^2 \times \mathbb{S}^2$  is possible.

Now, let us find the 4-dimensional reduced action to check the stability of vacua with the constant warping factor  $e^{2f}$ . We propose the following ansatz to deal with the size of extra dimensions dynamically:

$$\begin{aligned} ds^2 = & g_{\mu\nu}dx^\mu dx^\nu + L^2 e^{2f_1(x)} h_{ab}^{(1)}(y) dy_1^a dy_1^b + L^2 e^{2f_2(x)} h_{cd}^{(2)}(y) dy_2^c dy_2^d, \\ A = & A_a(y) dy^a = \left( -\frac{H_1}{2} \cos\theta_1 d\phi_1 - \frac{H_2}{2} \cos\theta_2 d\phi_2 \right) \tau^3, \quad \mathcal{A} = \mathcal{A}_\mu(x) dx^\mu, \end{aligned} \quad (2.31)$$

where  $h_{ab}^{(i)}$  is the metric of  $i$ -th sphere with the unit curvature radius. With the above ansatz and action, we can partially integrate out the extra dimension part of the original action as follows:

$$\begin{aligned} S_{\text{tot}} = & S_{\text{gravity}} + S_{\text{gauge}} \\ = & \frac{1}{2\kappa_4^2} \int d^4x \sqrt{-g} \left[ e^{2(f_1+f_2)} \left( \mathcal{R} - \frac{2\mathbf{s}}{L^2} - \ell_e^2 \mathcal{F}_{\mu\nu} \mathcal{F}^{\mu\nu} \right) \right. \\ & + 2e^{2(f_1+f_2)} (\nabla_\mu f_1 \nabla^\mu f_1 + \nabla_\mu f_2 \nabla^\mu f_2 + 4\nabla_\mu f_1 \nabla^\mu f_2) \\ & \left. + \frac{1}{2L^2} e^{2f_1} + \frac{1}{2L^2} e^{2f_2} - \frac{\ell_{H_1}^2}{2L^4} e^{2(f_2-f_1)} - \frac{\ell_{H_2}^2}{2L^4} e^{2(f_1-f_2)} \right], \end{aligned} \quad (2.32)$$

where  $2\kappa_4^2 = \frac{16\pi\mathbf{G}_{(s)}}{\mathcal{V}_1\mathcal{V}_2}$  with  $\mathcal{V}_i = \int d^2y_i L^2 \sqrt{h^{(i)}}$  and we took  $R[h_{ab}^{(i)}] = 1/2$ . In addition, the length parameter  $\ell_{H_i}$  is defined as  $\ell_{H_i}^2 \equiv \frac{\pi\mathbf{G}_{(s)}H_i^2}{4g_{\text{YM}}^2}$ . When  $H_1 = H_2$  and  $f_1 = f_2 = f$ ,

this reduced action becomes the same as the  $\mathbb{S}^4$  case (2.10). With a Weyl transformation,  $g_{\mu\nu} = e^{-2(f_1+f_2)}\tilde{g}_{\mu\nu}$ , the action takes the following form:

$$\mathcal{I} = \frac{1}{2\kappa^2} \int d^4x \sqrt{-\tilde{g}} \left[ \tilde{\mathcal{R}} - \ell_e^2 e^{2(f_1+f_2)} \tilde{\mathcal{F}}_{\mu\nu} \tilde{\mathcal{F}}^{\mu\nu} - 4 \left( \tilde{\nabla}_\mu f_1 \tilde{\nabla}^\mu f_1 + \tilde{\nabla}_\mu f_1 \tilde{\nabla}^\mu f_2 + \tilde{\nabla}_\mu f_2 \tilde{\nabla}^\mu f_2 \right) - V(\mathcal{X}_1, \mathcal{X}_2) \right], \quad (2.33)$$

where the potential is given by

$$V(\mathcal{X}_1, \mathcal{X}_2) = \frac{2\mathbf{s}}{L^2} \frac{1}{\mathcal{X}_1 \mathcal{X}_2} - \frac{1}{2L^2} \frac{1}{\mathcal{X}_1^2 \mathcal{X}_2} - \frac{1}{2L^2} \frac{1}{\mathcal{X}_1 \mathcal{X}_2^2} + \frac{\ell_{H_1}^2}{2L^4} \frac{1}{\mathcal{X}_1^3 \mathcal{X}_2} + \frac{\ell_{H_2}^2}{2L^4} \frac{1}{\mathcal{X}_1 \mathcal{X}_2^3}, \quad (2.34)$$

where  $\mathcal{X}_1$  and  $\mathcal{X}_2$  denote  $e^{2f_1}$  and  $e^{2f_2}$ , respectively. The potential  $V(\mathcal{X}_1, \mathcal{X}_2)$  characterizes the vacuum structure of this compactification. Some of the extrema of the potential gives the stable vacua. When  $f_1 = f_2$  and  $H_1 = H_2$ , this potential becomes the same potential as the  $\mathbb{S}^4$  case. We focus on this case. However, extending the extra dimensions with different sizes of  $\mathbb{S}^2$ 's is possible.

### 3 Thermodynamic Volume and Phase Diagram with Extra Dimensions

This section describes possible phase transitions of the system (2.11) based on the thermodynamic volume in the context of the black hole chemistry. Then, we scrutinize how the extra dimensions affect the phase transitions.

#### 3.1 Schwarzschild black hole

We start with the phase transition associated with the Schwarzschild-AdS black hole. It is well known that there is the Hawking-Page phase transition between the thermal AdS and Schwarzschild-AdS black hole. The metric of the black hole is given by

$$ds^2 = -U(r)dt^2 + r^2 (d\theta^2 + \sin^2 \theta d\varphi^2) + \frac{dr^2}{U(r)}, \quad (3.1)$$

where

$$U(r) = 1 - \frac{2\mathbf{G}_4 M}{r} - \frac{\tilde{\Lambda}_{\text{eff}}}{3} r^2. \quad (3.2)$$

The effective cosmological constant is given by  $\tilde{\Lambda}_{\text{eff}} = V(\mathcal{X}_s)/2 = \frac{\ell_H^2 + L^2(2\mathbf{s}\mathcal{X}_s^2 - \mathcal{X}_s)}{6L^4\mathcal{X}_s^4}$ , where  $\mathcal{X}_s$  is the stable size of the extra dimensions,  $e^{2f}$ . Furthermore, one can find a more convenient expression using the equation of motion  $\partial_{\mathcal{X}} V|_{\mathcal{X}=\mathcal{X}_s} = 0$ . The convenient form of the cosmological constant is

$$\tilde{\Lambda}_{\text{eff}} = \frac{4\mathbf{s}\mathcal{X}_s - 1}{8L^2\mathcal{X}_s^3}. \quad (3.3)$$

Now, we summarize the extended thermodynamics of black holes with the above cosmological constant as a thermodynamic pressure. See [18] for a pedagogical review. Important

quantities of the Schwarzschild-AdS black hole, entropy, temperature, and mass parameter can be written as

$$S = \frac{\pi r_h^2}{\mathbf{G}_4}, \quad T = \frac{1}{4\pi} \left( \frac{1}{r_h} - 3 \frac{\tilde{\Lambda}_{\text{eff}}}{3} r_h \right), \quad M = \frac{1}{\mathbf{G}_4} \left( \frac{r_h}{2} - \frac{1}{2} \frac{\tilde{\Lambda}_{\text{eff}}}{3} r_h^3 \right), \quad (3.4)$$

where the  $r_h$  is the horizon radius. For black hole chemistry, it is important to define the thermodynamic pressure given by

$$P_{\text{th}} = -\frac{\tilde{\Lambda}_{\text{eff}}}{8\pi \mathbf{G}_4}. \quad (3.5)$$

Then, one can derive the first law of the black hole thermodynamics as follows:

$$\delta M = T\delta S + V_{\text{th}}\delta P_{\text{th}}, \quad (3.6)$$

where the thermodynamic volume  $V_{\text{th}}$  is defined as  $V_{\text{th}} \equiv \frac{4}{3}\pi r_h^3$ . Also, there is the Smarr relation among thermodynamic quantities as follows:

$$M = 2ST - 2P_{\text{th}}V_{\text{th}}. \quad (3.7)$$

To find the internal energy, the variation (3.6) can be rearranged as follows:

$$\delta(M - V_{\text{th}}P_{\text{th}}) = T\delta S - P_{\text{th}}\delta V_{\text{th}}. \quad (3.8)$$

This implies that the internal energy is given by  $\mathcal{E} = M - V_{\text{th}}P_{\text{th}}$ , and one can notice that the black hole mass is not the internal energy but the enthalpy, which can be written as

$$M = \mathcal{E} + V_{\text{th}}P_{\text{th}}. \quad (3.9)$$

Also, the Gibbs free energy  $\mathcal{G}$  is a relevant thermodynamic potential for the  $(P_{\text{th}}, T)$  phase space. The form of the free energy is given by

$$\mathcal{G} = \mathcal{E} + P_{\text{th}}V_{\text{th}} - ST = M - ST. \quad (3.10)$$

The expression of  $P_{\text{th}}$  in terms of the thermodynamic volume and temperature is useful to understand the phase structure. Using the specific volume defined by  $v \equiv \left(\frac{6V_{\text{th}}}{\pi}\right)^{1/3} = 2r_h$ , the pressure can be written as follows:

$$P_{\text{th}} = \frac{1}{\mathbf{G}_4} \left( \frac{T}{v} - \frac{1}{2\pi v^2} \right). \quad (3.11)$$

The thermodynamic system has an instability in the region with  $\frac{\partial P_{\text{th}}}{\partial v} > 0$ . Thus, solutions with  $v < \frac{1}{\pi T}$  are thermodynamically unstable. This thermodynamic instability implies the well-known Hawking-Page transition. The  $(P_{\text{th}} - v)$  diagram is plotted to the left of Figure 2. This was studied in other previous works such as [18].

The Gibbs free energy of the Schwarzschild black hole is plotted in the right of Figure 2. Also, another saddle of the same theory exists without charge and angular momentum. This

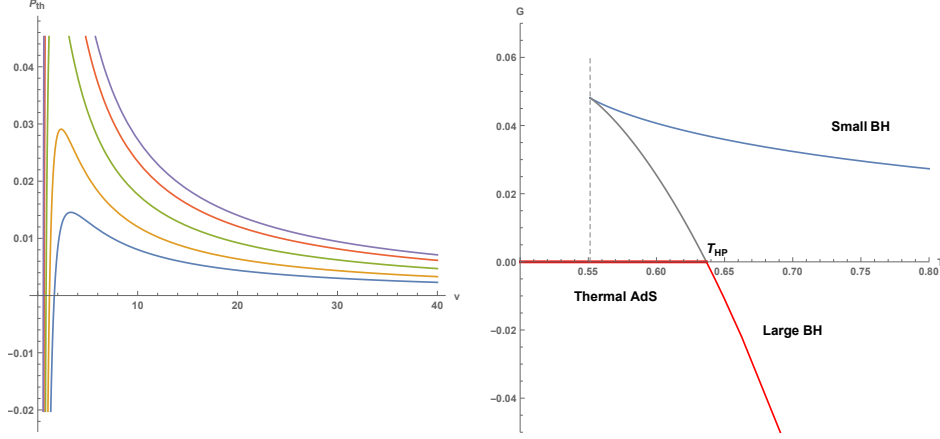


**Figure 2.  $P_{\text{th}} - v$  curve (Left):** The thermodynamic pressure curves shows the small black holes with  $v < \frac{1}{\pi T}$  are unstable. We set  $\mathbf{G}_4 = 1$  for simplicity. Upper curves describe pressures at higher temperatures.

**The Gibbs free energy of black holes and thermal AdS(Right):** This gravity system undergoes a phase transition between thermal AdS and large black holes. It occurs when the Gibbs free energy of black holes is (approximately) zero. The red curve shows that this phase transition is first order.

saddle is the thermal AdS and has approximately zero free energy. Therefore, the Hawking-Page transition occurs when the free energy almost vanishes, equivalently, when  $P_{\text{th}} = \frac{3\pi T^2}{8}$ . In Section 2, we related the size of the extra dimension (or instanton number) to the effective cosmological constant, in the extended phase space context, the thermodynamic pressure  $P_{\text{th}}$ . So we can get the phase transition curves for  $\mathbf{s} = -1, 0$  (Left of Figure 3) and  $\mathbf{s} = +1$  (Right of Figure 3) in terms of the extra dimension size. In addition, we obtain the restricted black hole size due to the Hawking-Page transition. The result is shown in Figure 4. The figures on the right contain the de Sitter black hole region. The thermodynamic stability cannot be applied to this de Sitter case. The de Sitter case is beyond the scope of the present work.

### 3.2 Dyonic black hole with $q = B$

In this section, as a generalization to the previous neutral black hole case, we consider charged black holes with a constant extra dimension size. This situation is governed by (2.13) and (2.14) as we discussed. To find black hole solutions, we propose the following form of metric and gauge fields:

$$ds^2 = -U(r)dt^2 + r^2 (d\theta^2 + \sin^2 \theta d\varphi^2) + \frac{dr^2}{U(r)}$$

$$\tilde{A} = \tilde{A}_t(r)dt + B \cos \theta d\varphi. \quad (3.12)$$

By solving the equations of motion and imposing the constraint (2.14), we obtain a dyonic black hole solution given by

$$U(r) = 1 - \frac{2\mathbf{G}_4 M}{r} - r^2 \frac{\tilde{\Lambda}_{\text{eff}}}{3} + \frac{2q^2 \ell_e^2}{r^2}, \quad \tilde{A}_t(r) = \left( \frac{\mathbf{G}_4}{\ell_e^2} \mu - \frac{q}{r} \right), \quad B = q, \quad (3.13)$$

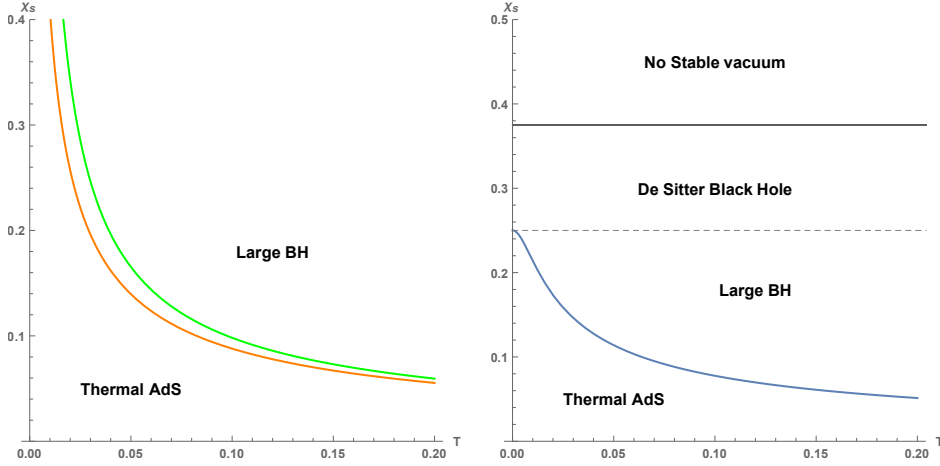


**Figure 3. Phase diagram in terms of the extra dimension size :** The left figure is for  $s = -1$  and 0 cases, and the right is for  $s = +1$ . We set  $1/(64\pi\mathbf{G}_4L^2) = 0.02$ .

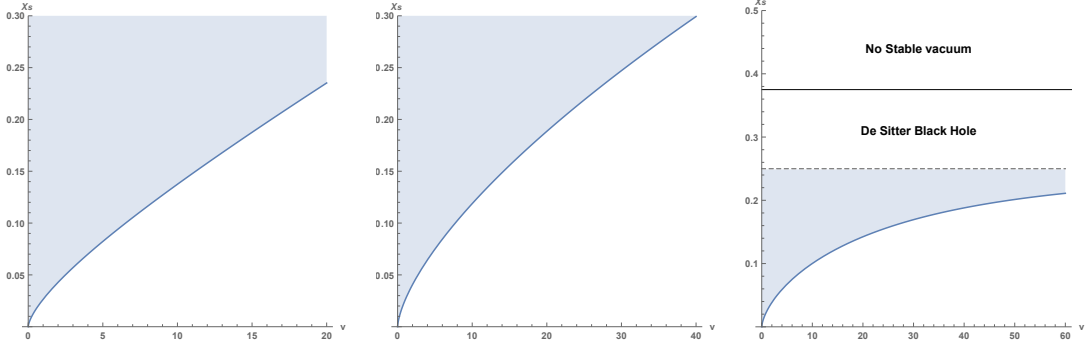


**Figure 4. Disallowed black hole sizes:** Colored regions describe the sizes of black holes that cannot exist. Figures correspond to  $s = -1, 0,$  and  $+1$  from the left to the right. We set  $1/(64\pi\mathbf{G}_4L^2) = 0.02$ . The disallowed size region gets wider as the extra dimension size increases. We leave the de Sitter region as a white blank.

where  $\tilde{\Lambda}_{\text{eff}}$  is given by (3.3).

Due to the magnetic field contribution, this dyonic black hole has a non-normalizable gauge field configuration. Still, this solution has a well-defined thermodynamics. Therefore, we will construct the extended thermodynamics with the thermodynamic pressure and volume. From the holographic viewpoint, the magnetic field corresponds to an external field to the boundary (2+1)-dimensional system. Therefore, the non-normalizable gauge field is natural as it originates from the external field in the dual system. In addition, one can find the physical meaning of the constraint,  $q = B$ , through the holographic interpretation. The holographic interpretation of  $q$  and  $B$  are the density and the external magnetic flux in the (2+1)-dimensional system. An easy way to introduce this constraint is to consider the abelian Chern-Simons theory. The Gauss constraint of such a Chern-Simons theory is given by  $B = kq$ , where  $k$  is the Chern-Simons level. Therefore, this dyonic black hole can be identified with a dual bulk system to a Chern-Simons system with

level  $k = 1$ .

Let us come back to thermodynamics. Necessary thermodynamic quantities for this black hole are entropy, temperature, and black hole mass as follows:

$$S = \frac{\pi r_h^2}{\mathbf{G}_4}, \quad T = \frac{1}{4\pi} \left( \frac{1}{r_h} - 3r_h \frac{\tilde{\Lambda}_{\text{eff}}}{3} - \frac{2q^2 \ell_e^2}{r_h^3} \right), \quad M = \frac{1}{\mathbf{G}_4} \left( \frac{r_h}{2} - \frac{1}{2} \frac{\tilde{\Lambda}_{\text{eff}}}{3} r_h^3 + \frac{q^2 \ell_e^2}{r_h} \right). \quad (3.14)$$

In addition, we define again the thermodynamic pressure given by (3.5). Then, one can derive the variation of the mass parameter as follows:

$$\delta M = T\delta S + \mu\delta q - \mathcal{M}\delta B + V_{\text{th}}\delta P_{\text{th}}, \quad (3.15)$$

where the chemical potential  $\mu$ , magnetization  $\mathcal{M}$  and thermodynamic volume  $V_{\text{th}}$  are defined as

$$\mu = \frac{\ell_e^2}{\mathbf{G}_4} \frac{q}{r_h}, \quad \mathcal{M} = -\frac{\ell_e^2}{\mathbf{G}_4} \frac{B}{r_h} = -\frac{\ell_e^2}{\mathbf{G}_4} \frac{q}{r_h}, \quad V_{\text{th}} = \frac{4}{3}\pi r_h^3, \quad (3.16)$$

where we demand  $B = q$  always. Also, the Smarr relation can be written as follows<sup>3</sup>:

$$M = 2ST - 2P_{\text{th}}V_{\text{th}} + 2q\mu = 2ST - 2P_{\text{th}}V_{\text{th}} + q\mu - \mathcal{M}B. \quad (3.17)$$

The variation (3.15) is rearranged to make clear the internal energy and the first law as follows:

$$\delta(M - V_{\text{th}}P_{\text{th}} + \mathcal{M}B) = T\delta S + \mu\delta q - P_{\text{th}}\delta V_{\text{th}} + B\delta\mathcal{M} \quad (3.18)$$

Therefore, the internal energy is given by

$$\mathcal{E} = M - V_{\text{th}}P_{\text{th}} + \mathcal{M}B. \quad (3.19)$$

Thus, the black hole mass

$$M = \mathcal{E} + V_{\text{th}}P_{\text{th}} - \mathcal{M}B, \quad (3.20)$$

is not the internal energy but the enthalpy with magnetic subtraction. We will consider the canonical ensemble with the fixed charge and magnetic field. The Gibbs free energy is the relevant thermodynamic potential in this ensemble. The expression for the Gibbs free energy is

$$\mathcal{G} = \epsilon + P_{\text{th}}V_{\text{th}} - ST - \mathcal{M}B = M - ST \quad (3.21)$$

Now, we rewrite the thermodynamic pressure in terms of the temperature and the specific volume<sup>4</sup> as follows:

$$P_{\text{th}} = \frac{1}{\mathbf{G}_4} \left( \frac{4q^2 \ell_e^2}{\pi v^4} - \frac{1}{2\pi v^2} + \frac{T}{v} \right). \quad (3.22)$$

<sup>3</sup>See [54] for a different variation of the Smarr relation.

<sup>4</sup>We employ the specific volume defined as  $v \equiv \left(\frac{6V_{\text{th}}}{\pi}\right)^{1/3} = 2r_h$  as we mentioned earlier.

This expression shows a well-known Large/Small black hole phase transition [5]. The only difference from the original work is that the charge is doubled due to the magnetic charge.

To analyze this thermodynamic system with a nonvanishing charge, we introduce a convenient choice of the thermodynamic variables given by

$$v = ql_e \bar{v}, \quad T = \frac{\bar{T}}{2\pi ql_e}, \quad P_{\text{th}} = \frac{\bar{P}}{\pi \mathbf{G}_4 q^2 \ell_e^2}, \quad \mathcal{G} = \frac{ql_e \bar{\mathcal{G}}}{8\mathbf{G}_4}. \quad (3.23)$$

Then, we have

$$\bar{P} = \frac{4}{\bar{v}^4} - \frac{1}{2\bar{v}^2} + \frac{\bar{T}}{2\bar{v}}, \quad \bar{T} = 2\bar{P}\bar{v} + \frac{1}{\bar{v}} - \frac{8}{\bar{v}^3}, \quad \bar{\mathcal{G}} = \frac{24}{\bar{v}} + \bar{v} - \frac{2\bar{P}\bar{v}^3}{3}. \quad (3.24)$$

The typical pressure shapes are plotted in Figure 5 using the above expressions. The  $(\bar{P}-\bar{v})$  diagram in the figure can be compared to that of the Van de Waals fluid.

To have the large to small black hole phase transition,  $(\bar{P}-\bar{v})$  diagram in Figure 5 implies that the pressure should have two extrema. Therefore, the following equation should have two roots for  $\bar{v}$ :

$$\bar{v}^5 \partial_{\bar{v}} \bar{P} = -16 + \bar{v}^2 \left( 1 - \frac{\bar{T}}{2\bar{v}} \right) = 0. \quad (3.25)$$

The condition for two roots is given by

$$1/3\sqrt{3} > \bar{T}. \quad (3.26)$$

On the other hand, the Gibbs free energy  $\bar{\mathcal{G}}$  should have two extrema for the swallow tail. One can easily see that the condition is

$$1/192 > \bar{P}. \quad (3.27)$$

Therefore, the critical point is given by  $(\bar{T}_c, \bar{P}_c) = (1/3\sqrt{3}, 1/192)$ . We plot the Gibbs free energy  $\bar{\mathcal{G}}$  in Figure 5. In addition, one can find a phase boundary using a numerical method. The phase diagram is shown in Figure 6. The boundary curve is similar to the RN black hole case [5] except for magnetic charge contribution.

Now, we find the connection between the thermodynamic pressure and the extra dimension size. The size of the extra dimension can be represented by the warping factor  $L^2 e^{2f} = L^2 \mathcal{X}$ . For the  $\mathbf{s} = 0$  case,  $L$  represents just a length unit. Thus, one may set  $L$  and 1. On the other hand,  $L^2$  is the length scale of the cosmological constant for the cases with  $\mathbf{s} = \pm 1$ . The effective cosmological constant can be written by the potential as follows:

$$\tilde{\Lambda}_{\text{eff}} = V(\mathcal{X}_s)/2 = \frac{4\mathbf{s}\mathcal{X}_s - 1}{8L^2 \mathcal{X}_s^3}, \quad (3.28)$$

where we used an equation of motion,  $\partial_{\mathcal{X}_s} V = 0$ , and  $\mathcal{X}_s$  denotes the dimensionless size of the extra dimensions. The physical size is given by  $\mathcal{X}_s L^2$ . Thus the pressure expression in



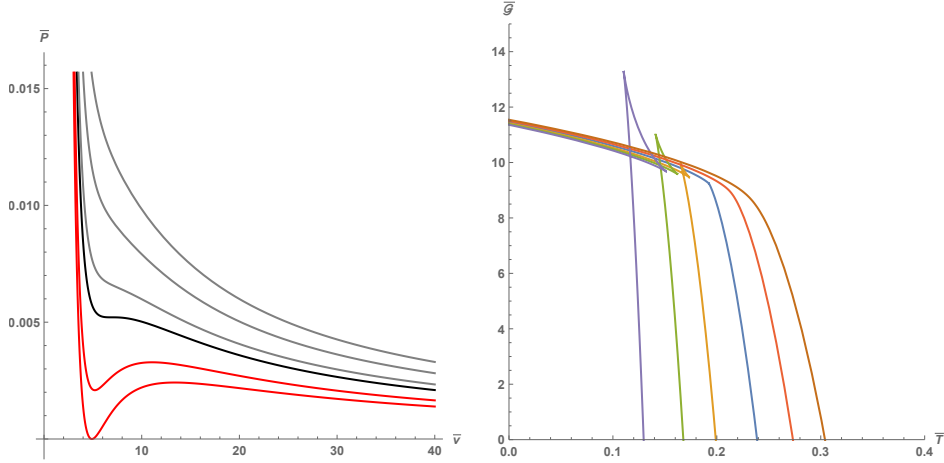


**Figure 5. Thermodynamic pressure  $\bar{P}(\bar{T}, \bar{v})$  (Left):** The convenient quantities absorbing charge parameter are defined in (3.23) and (3.24). Since the black hole solutions are unstable when  $d\bar{P}/d\bar{v} > 0$ , the Large/Small black hole phase transition can happen. We set  $\bar{T} = (\frac{0.4}{3\sqrt{3}}, \frac{1}{3\sqrt{6}}, \frac{1}{3\sqrt{3}}, \frac{1.3}{3\sqrt{3}}, \frac{1.5}{3\sqrt{3}})$  from the highest curve to the lowest curve. **The Gibbs free energy (Right):** This figure shows the appearance of the swallowtail by lowering the thermodynamic pressure ( $\bar{P}$ ). We set  $\bar{P} = (\frac{0.3}{192}, \frac{0.5}{192}, \frac{0.7}{192}, \frac{1}{192}, \frac{1.3}{192}, \frac{1.6}{192})$  from the purple curve to the brown curve.

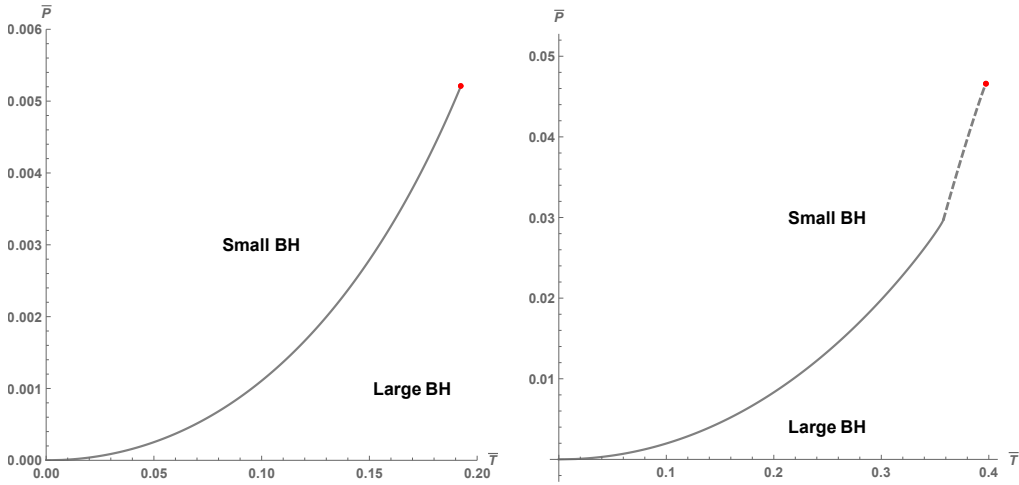


**Figure 6. Phase diagrams of the dyonic black hole and the Kerr-AdS black hole:** The left and right figures show the phase diagrams for the dyonic black hole with  $q = B$  and the rotating black hole, respectively. They show the Large/Small black hole transitions. The red dots denote the critical points. The dyonic case demonstrates the typical first-order phase transition for AdS black holes. On the other hand, a zeroth-order phase transition shows up near the critical point in the rotating black hole case. The dashed line represents the phase boundary curve for the zeroth-order phase transition.

terms of the extra-dimension size is given by  $\bar{P} = \gamma^3 \frac{1-4s\chi_s}{\chi_s^3} = \frac{q^2 \ell_e^2}{64L^2} \frac{1-4s\chi_s}{\chi_s^3}$ . By inverting

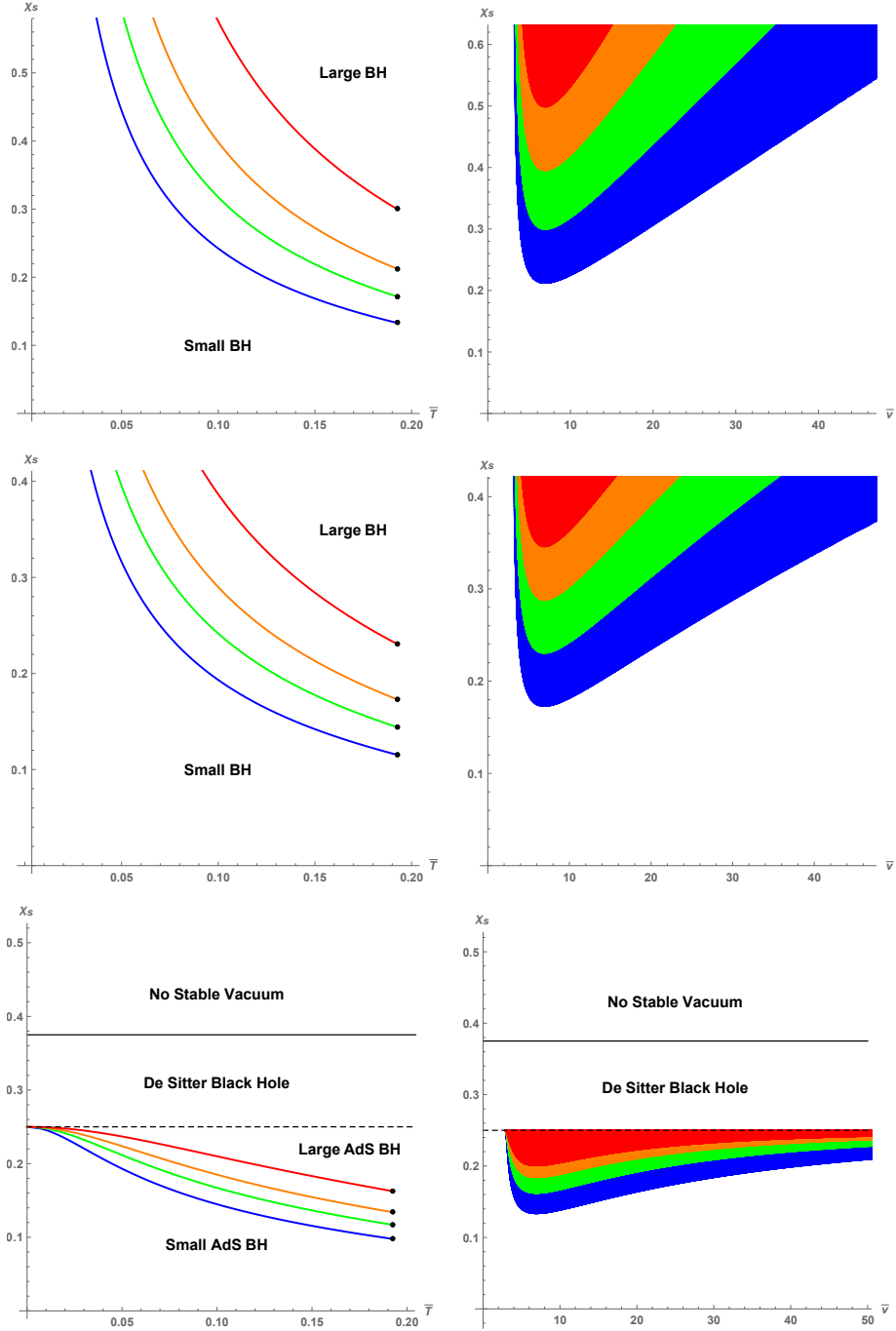


**Figure 7.** From top to bottom, we depict  $s = -1, 0,$  and  $+1$  cases, respectively. The left figures are the phase diagram with the extra-dimension size. The right figures show the disallowed range of the horizon size  $\bar{v} = 2r_h/(q\ell_e)$ . From the red curve or region to the blue curve or region, we use  $\gamma = (0.06, 0.05, 0.04, 0.03)$  shown in (3.2).

this relation, one can obtain the dimensionless size given by

$$\mathcal{X}_s = \frac{\gamma \left( 2^{1/3} \left( \sqrt{81\bar{P} + 768\gamma^3 s} + 9\sqrt{\bar{P}} \right)^{2/3} - 8 \cdot 3^{1/3} \gamma s \right)}{6^{2/3} \sqrt{\bar{P}} \left( \sqrt{81\bar{P} + 768\gamma^3 s} + 9\sqrt{\bar{P}} \right)^{1/3}}. \quad (3.29)$$

This formula helps us construct the phase diagrams for  $\mathbf{s} = 0, \pm 1$  cases. We provide them in Figure 7. Also, we find thermodynamically unstable size-parameter regions for each phase diagram curve. The right ones in Figure 7 show these disallowed parameter regions.

Notably, each curve for the phase boundaries provides the disallowed size range of black holes. These ranges give us information about the size of the extra dimensions. We plot the disallowed size range in Figure 7. The larger extra dimensions prevent a larger range of black hole sizes. To form black holes easily, the extra-dimension size should be small enough. The bottom figures of Figure 7 demonstrates  $\mathbf{s} = +1$  (i.e., a positive  $\Lambda$ ) case. As one can see, there is a transition between the de Sitter geometries and the AdS dyonic black hole geometries. Near the  $\mathcal{X}_s = 1/4$  from the AdS region, almost all sizes of the black hole are disallowed. It would be interesting to study what happens near this critical extra-dimension size.

### 3.3 Kerr-AdS black hole

In this section, we study the black hole chemistry of the 4-dimensional Kerr-AdS black hole affected by extra-dimension dynamics. The metric is given by

$$ds^2 = -\frac{\Delta_r}{\rho^2} \left( dt - \frac{a \sin^2 \theta}{\Xi} d\phi \right)^2 + \frac{\rho^2}{\Delta_r} dr^2 + \frac{\rho^2}{\Delta_\theta} d\theta^2 + \frac{\sin^2 \theta \Delta_\theta}{\rho^2} \left( a dt - \frac{r^2 + a^2}{\Xi} d\phi \right)^2, \quad (3.30)$$

where

$$\rho^2 = r^2 + a^2 \cos^2 \theta, \quad \Delta_r = (r^2 + a^2) \left( 1 - \frac{\tilde{\Lambda}_{\text{eff}}}{3} r^2 \right) - 2G_4 m r, \quad (3.31)$$

$$\Xi = 1 + \frac{\tilde{\Lambda}_{\text{eff}}}{3} a^2, \quad \Delta_\theta = 1 + \frac{\tilde{\Lambda}_{\text{eff}}}{3} a^2 \cos^2 \theta. \quad (3.32)$$

The  $\tilde{\Lambda}_{\text{eff}}$  is related to the potential (2.12) as  $V(\mathcal{X}_s) = 2\tilde{\Lambda}_{\text{eff}}$ , where  $\mathcal{X}_s$  is the stable size of the extra dimensions, as we mentioned.

The mass  $M$  and the angular momentum  $J$  are related to the parameters  $m$  and  $a$  via

$$M = \frac{m}{\Xi^2}, \quad J = \frac{am}{\Xi^2}. \quad (3.33)$$

Here,  $m$  can be represented by other parameters since the metric satisfies  $\Delta_r(r_+) = 0$  with the event horizon  $r_+$ . Thus, one can rewrite the mass and the angular momentum as follows:

$$M = \frac{1}{2G_4 \Xi^2 r_+} \left( a^2 + r_+^2 - \frac{1}{3} r_+^2 (a^2 + r_+^2) \tilde{\Lambda}_{\text{eff}} \right), \quad (3.34)$$

$$J = \frac{a}{2G_4 \Xi^2 r_+} \left( a^2 + r_+^2 - \frac{1}{3} r_+^2 (a^2 + r_+^2) \tilde{\Lambda}_{\text{eff}} \right).$$

The Hawking temperature of the Kerr-AdS black hole, the Bekenstein-Hawking entropy, and the angular speed are

$$T = \frac{r_+}{4\pi (a^2 + r_+^2)} \left( 1 - \frac{a^2}{r_+^2} - \frac{1}{3} (a^2 + 3r_+^2) \tilde{\Lambda}_{\text{eff}} \right), \quad S = \frac{\pi(r_+^2 + a^2)}{G_4 \Xi}, \quad \Omega' = \frac{a\Xi}{r_+^2 + a^2}, \quad (3.35)$$

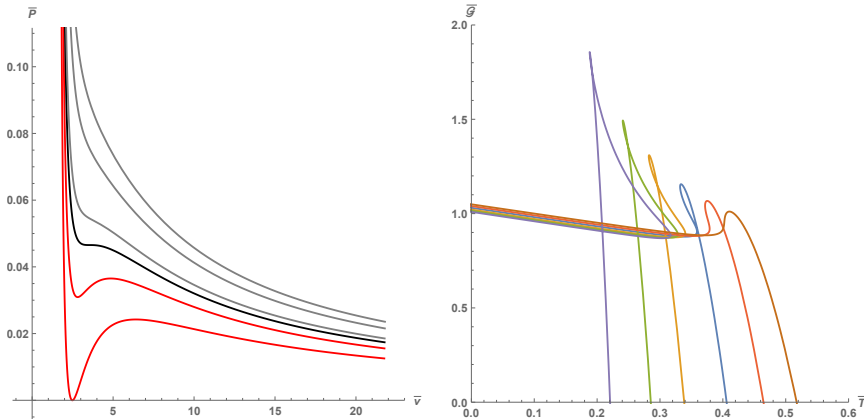


**Figure 8.** ( $\bar{P} - \bar{v}$ ) curve for Kerr-AdS black hole (Left): The black solid lines are the curves for  $\bar{T} \geq \bar{T}_c$ , and the red solid lines denote curves below the critical temperature  $\bar{T}_c$ . Since black holes are thermodynamically unstable when  $dP_{\text{th}}/dv > 0$ , the Large/Small black hole phase transition occurs. From the highest to the lowest curve, we set  $\bar{T} = (0.3, 0.36, 0.39, 0.42, 0.48, 0.52)$ .

**Gibbs free energy of Kerr-AdS black hole (Right):** The scaled Gibbs free energy  $\bar{\mathcal{G}}$  with fixed  $\bar{P}$  shows the cowboy's lassos rather than the swallowtails. This implies a zeroth-order phase transition happens in a specific  $\bar{P}$  range. From right to left curves, we set  $\bar{P} = (0.09, 0.015, 0.021, 0.03, 0.039, 0.048)$ .

respectively. In addition, the more appropriate angular speed for our case in a different frame is

$$\Omega = \Omega' - \frac{\tilde{\Lambda}_{\text{eff}}}{3} a. \quad (3.36)$$

We use this quantity to find the first law.

Now, we start with the identification (3.5) to find the extended thermodynamics or the black hole chemistry. Then, one can derive the first law by varying thermodynamic variables. The variation of the black hole mass is given by

$$\delta M = T\delta S + \Omega\delta J + V_{\text{th}}\delta P_{\text{th}}, \quad (3.37)$$

where

$$V_{\text{th}} = \frac{4\pi r_+^3}{3} \left( \frac{1 + \frac{a^2}{r_+^2}}{\Xi^2} \right) \left( 1 + \frac{1}{6} a^2 \tilde{\Lambda}_{\text{eff}} + \frac{a^2}{2r_+^2} \right). \quad (3.38)$$

This is the thermodynamic volume obtained in [6]. One may see that this expression becomes the thermodynamic volume (3.16) for the dyonic case in  $a \rightarrow 0$  limit. There is a conjecture about an inequality between this volume and the horizon area. See [4]. It would be interesting to find the role of this inequality in the black hole chemistry.

As a comment on the expression (3.38), the geometric meaning of the thermodynamic volume for the Kerr-AdS black hole is unclear. Like the charged black hole case<sup>5</sup>, one may

<sup>5</sup>It is known that the thermodynamic volume of the charged black hole is equal to the spatial volume inside the horizon,  $V_{\text{th}} = \int_0^{r_+} d^3x \sqrt{-g}$ . The dyonic black hole also obeys this geometrical meaning.

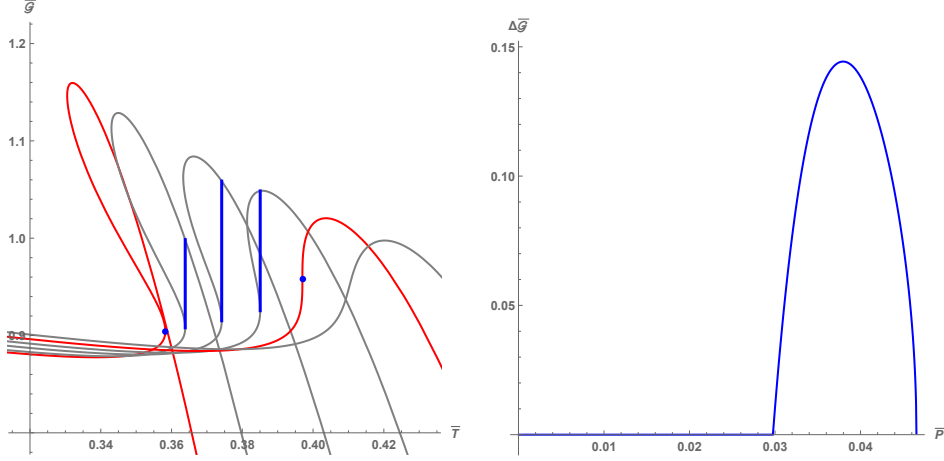


**Figure 9. Zoomed Gibbs free energy  $\bar{\mathcal{G}}$  around the transition (Left):** One can notice that a free energy jump occurs during the phase transition. The corresponding pressures  $\bar{P}$  are lower from the right to the left curve.

**Free energy gap (right):** The free energy gap between the large and small black holes.

represent this volume as a volume  $V_\Sigma$  surrounded by a surface  $\Sigma$ . By the axial symmetry, it is natural to define the location of  $\Sigma$  by  $r = r_+ \xi(\theta)$ . Then, the thermodynamic volume can be written as

$$V_{\text{th}} = \int_{V_\Sigma} d^3x \sqrt{-g} = \frac{4\pi r_+^3}{3} \int_{-1}^1 d\mathbf{p} \frac{1}{2\xi} \left[ \frac{a^2}{r_+^2} x^2 \xi(\mathbf{p}) + \xi(\mathbf{p})^3 \right], \quad (3.39)$$

where  $\mathbf{p} = \cos \theta$ , and  $\xi(\mathbf{p})$  is deduced by an even function due to the axial symmetry of the black hole. By comparing this with (3.38), we find the condition for  $\Sigma$  producing the thermodynamic volume as follows:

$$\int_{-1}^1 d\mathbf{p} \frac{1}{2} [\alpha \mathbf{p}^2 \xi(\mathbf{p}) + \xi(\mathbf{p})^3] = \frac{1 + \alpha}{1 + \beta} \left( 1 + \alpha + \frac{\beta}{2} \right), \quad (3.40)$$

where  $\alpha = \frac{a^2}{r_+^2}$  and  $\beta = \frac{1}{3} a^2 \tilde{\Lambda}_{\text{eff}}$ . Infinitely many  $\xi(\mathbf{p})$ 's fulfills the above condition. In the dyonic black hole case,  $\Sigma$  is nothing but its horizon surface. This is a natural consequence since the horizon surface is the only physically meaningful surface in the charged black hole geometry. Similarly, one may consider two physically meaningful surfaces in the Kerr-AdS black hole. One is the horizon again, and the other one is the surface of the ergosphere. Unfortunately, both two candidates can not be  $\Sigma$ . The horizon is too small, and the ergosphere is too big to produce (3.38). One possible surface is an averaged surface between the outer horizon and the ergosurface. However, we have no idea how to address this problem. More in-depth consideration of thermodynamics should be needed.

Now, let us come back to the black hole chemistry of the Kerr-AdS black hole. The internal energy of the system is again  $\mathcal{E} = M - P_{\text{th}} V_{\text{th}}$  due to the variation of the mass (3.37). In addition, the Gibbs free energy and its variation can be found as follows:

$$\mathcal{G} = M - ST \quad , \quad \delta \mathcal{G} = -S \delta T + V_{\text{th}} \delta P_{\text{th}} + \Omega \delta J. \quad (3.41)$$

Thus, the Gibbs free energy is the relevant thermodynamic potential describing the phase transitions in the  $(P_{\text{th}}-T)$  space with a fixed  $J$ .

Like the dyonic black hole case, we define convenient parameters with the nonvanishing rotation parameter  $a$ . They are defined as

$$\begin{aligned}\bar{r}_+ &= \frac{r_+}{a}, \quad \bar{T} = 4\pi a T, \quad \bar{P} = 8\pi \mathbf{G}_4 a^2 P_{\text{th}}, \\ \bar{V} &= \frac{V_{\text{th}}}{2\pi a^3}, \quad \bar{\mathcal{G}} = \frac{\mathbf{G}_4}{a} \mathcal{G}, \quad \bar{v} = \left(\frac{6\bar{V}}{\pi}\right)^{1/3},\end{aligned}\tag{3.42}$$

where  $\bar{v}$  is based on the specific volume,  $v = \left(\frac{6V_{\text{th}}}{\pi}\right)^{1/3}$ . Employing the above parametrization, we find the expressions absorbing  $a$  for the specific volume, pressure, and Gibbs free energy as follows:

$$\begin{aligned}\bar{v} &= \left(\frac{2}{\pi}\right)^{1/3} \bar{r}_+ \left(\frac{\bar{r}_+ (3\bar{r}_+^2 + 1) (6\bar{r}_+ - \bar{T})}{(\bar{r}_+ \bar{T} - 3\bar{r}_+^2 + 1)^2}\right)^{1/3} \\ \bar{P} &= \frac{3(\bar{r}_+^3 \bar{T} + \bar{r}_+ \bar{T} - \bar{r}_+^2 + 1)}{3\bar{r}_+^4 + \bar{r}_+^2} \\ \bar{\mathcal{G}} &= \frac{\bar{P}^2 (3\bar{r}_+^4 + \bar{r}_+^2) - 3\bar{P} (\bar{r}_+^2 - 1)^2 + 9(\bar{r}_+^2 + 3)}{4(\bar{P} - 3)^2 \bar{r}_+}.\end{aligned}\tag{3.43}$$

This set of formulas is enough to find the  $(\bar{P} - \bar{v})$  curves and the Gibbs free energy  $\bar{\mathcal{G}}$  graph. They are shown in Figure 8. From the figure, one can notice that the Gibbs free energy behavior of the Kerr-AdS black hole differs from that of the dyonic black hole or the RN black hole. The curves of the Gibbs free energy look like cowboy's lassos. This implies that the zeroth-order phase transition may occur. The left zoomed figure in Figure 9 proves this occurrence. Also, the right one of Figure 9 demonstrates the free energy gap showing the zeroth order phase transition.

The mathematical origin of the difference between the swallowtail of dyonic black hole and the cowboy's lasso of Kerr-AdS black hole originates from the number of roots for  $\frac{\partial \bar{\mathcal{G}}}{\partial \bar{r}_+} = 0$  and  $\frac{\partial \bar{T}}{\partial \bar{r}_+} = 0$ . Both equations have the same real-positive roots for  $\bar{r}_+$  in the dyonic black hole case. Therefore, the number of roots of the two equations is identical for all values of  $\bar{P}$ . One can check by an explicit calculation as follows:

$$\bar{r}_+^4 \partial_{\bar{r}_+} \bar{T} = \bar{r}_+^2 \partial_{\bar{r}_+} \bar{\mathcal{G}} = -2\bar{P}^2 \bar{r}_+^4 + \bar{r}_+^2 - 24.\tag{3.44}$$

On the other hand, this coincidence does not happen in the Kerr-AdS black hole. This makes the form of Gibbs free energy a lasso shape.

Based on (3.43), one can construct the phase diagram of the 4-dimensional Kerr-AdS black hole by collecting data from Figure 8. The phase diagram is presented in the right graph of Figure 6. One can find the zeroth-order phase transition line near the critical point in the figure. The Large/Small black hole transition of the dyonic black hole is first-order, so the Gibbs free energy is continuous under the phase transition. However, the Kerr-AdS black hole shows the discontinuous Gibbs free energy under the phase transition. This

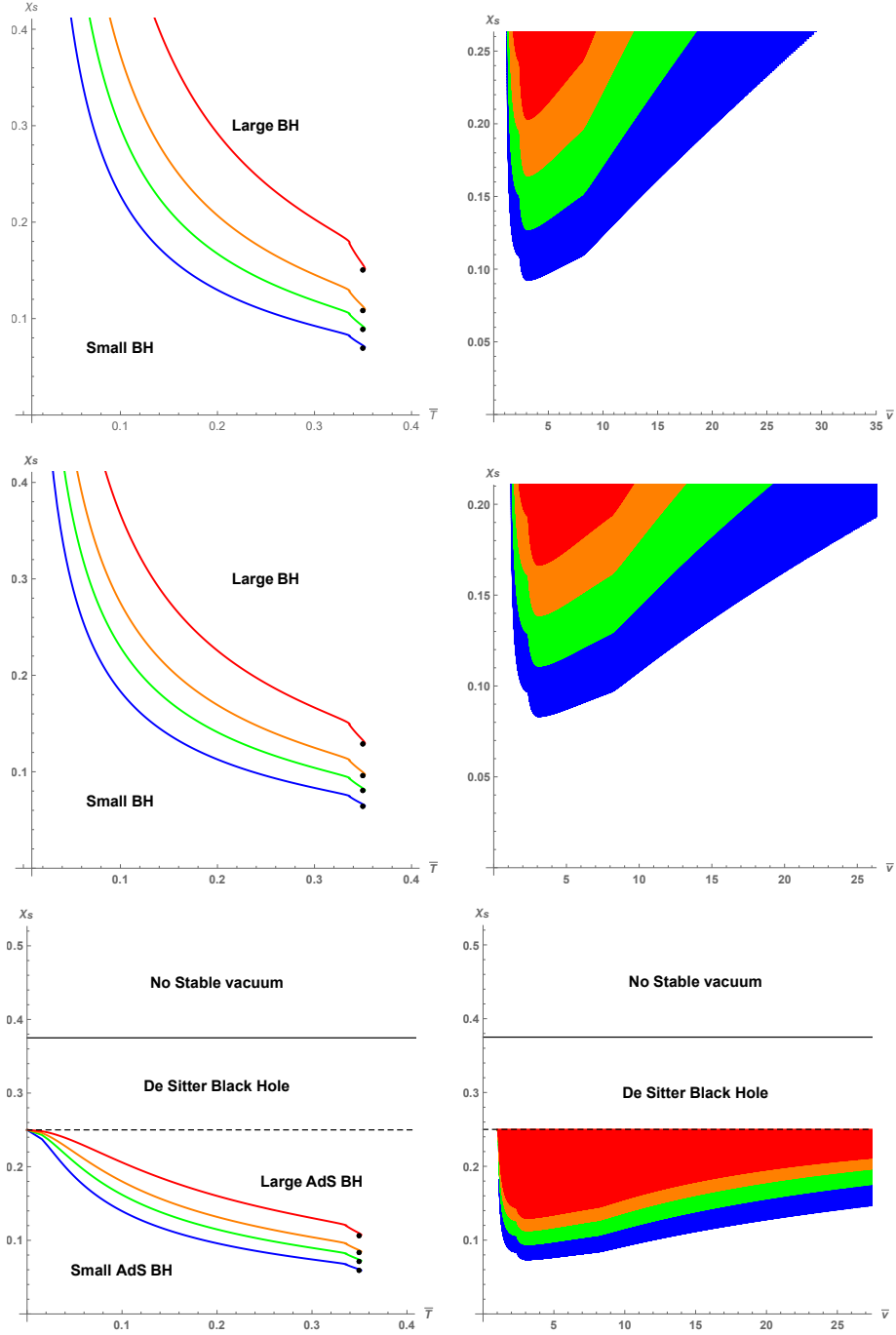


**Figure 10.** The three left figures are the phase diagrams regarding the extra-dimension size and temperature. The three figures on the right depict disallowed specific volumes,  $\bar{v}$ . From top to bottom, the figures correspond to the negative, vanishing, and positive  $\Lambda$ , equivalently,  $s = -1, 0, 1$  cases. From the red to blue curves, the charge parameters are given as  $\gamma = (a^2/(8L^2))^{1/3} = (0.06, 0.05, 0.04, 0.03)$ . The zeroth-order phase transition causes the bending shapes near the critical points (black dots).

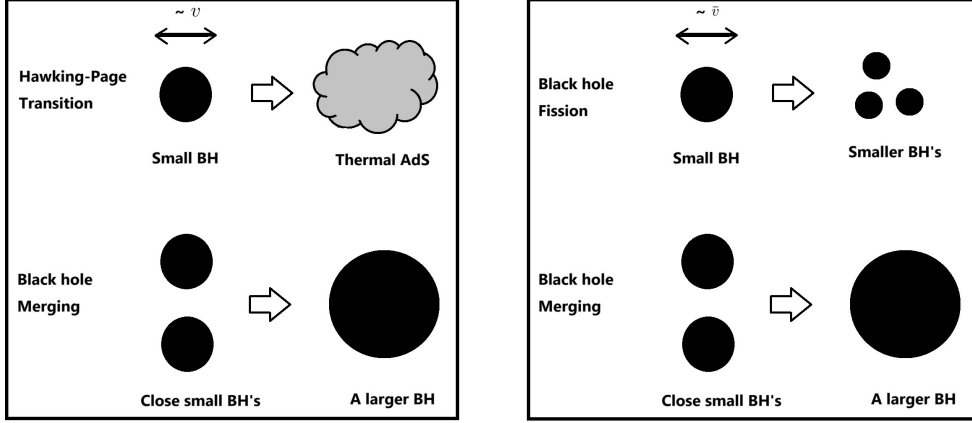


**Figure 11. Scenarios for Schwarzschild black hole (Left) and Dyonic or Kerr-AdS black hole (Right):** As the extra-dimension size increases, the Schwarz black hole transitions to the thermal AdS or merges with another black hole into a larger black hole. For the dyonic or Kerr-AdS black hole, the rough size of the black hole should be much smaller or larger. Therefore, the black hole fissions into smaller black holes or merges into a larger black hole.

zeroth-order phase borderline, denoted by a dashed line, appears near the critical point. See the right of Figure 6.

It would be valuable to clarify the physical meaning of this zeroth-order phase transition in the context of AdS/CFT. Unfortunately, we don't have a good explanation. This must be related to the strongly coupled ABJM theory on  $\mathbb{S} \times \mathbb{S}^2$ . The holographic interpretation of the black hole chemistry has been studied recently. See [38] for a review. Also, one may construct that of the five-dimensional Kerr-AdS black hole and examine how this phenomenon is related to the  $\mathcal{N} = 4$  super Yang-Miils theory.

Now, let us see how the extra-dimension size is related to the phase transition and black hole sizes. Using (3.28), It is possible to convert the phase diagram presented on the right of Figure 6 into phase diagrams in terms of the extra dimension size. See Figure 10. We use the scaled pressure expression given by  $\bar{P} = \gamma^3 \left( \frac{1-4s\mathcal{X}_s}{\mathcal{X}_s^3} \right)$  with  $\gamma^3 = a^2/(8L^2)$  in the figure. The left figures show the phase boundaries with the critical points. As can be seen in the figures, the phase boundaries suddenly bend near the critical points denoted by black dots. This behavior is due to the zeroth-order phase transition. In addition, the right figures of Figure 10 show the disallowed specific volume parameter  $\bar{v}$  by thermodynamic instability.

### 3.4 Black hole merging and fission with large extra dimensions

The thermodynamic volume  $V_{\text{th}}$  or the specific volume  $v$  is given by a scale of horizon size. Roughly speaking,  $v$  is almost the radius of a black hole horizon. On the other hand, the thermodynamic pressure  $P_{\text{th}}$  is determined by the effective cosmological constant, which depends on the extra-dimension size (or an instanton number) in our model. Therefore, the horizon size and the extra-dimension size are conjugate thermodynamic quantities of each other in our model.



Let us see what happens in the Schwarzschild case studied in section 3.1. From Figure 3 and 4, both the thermal AdS and black hole can exist for a given extra-dimension size  $\mathcal{X}_s$ . However, the black hole size  $v$  should be larger than critical values determined by the curves in Figure 4. As the extra-dimension size increases, the viable size of the black hole also increases. Therefore, a small black hole can take two scenarios. The first choice is a transition to the thermal AdS, i.e., a gas of gravitons. In addition, the second scenario is to merge with another small black hole to become a bigger one.

Meanwhile, the dyonic and Kerr-AdS black holes have large and small black hole phases. When the extra-dimension size  $\mathcal{X}_s$  is smaller than the critical points (Black dots in Figure 7 and 10), every black hole with whatever thermodynamic volume or specific volume  $\bar{v}$  is stable. As, however,  $\mathcal{X}_s$  grows and becomes larger than the critical points, the disallowed size region, denoted by the colored region in the figures on the right of Figure 7 and 10, also grows. A black hole with a size  $\bar{v}$  included in the colored regions becomes unstable. There are two cases of such a black hole. The first is a black hole with a high  $\bar{T}$ , and the other case is a black hole with a low  $\bar{T}$ . The high  $\bar{T}$  means a high temperature or large charge and angular momentum. Black holes with large  $\bar{T}$  tend to merge with other black holes to make a larger black hole. On the other hand, black holes with small  $\bar{T}$  tend to fission into smaller black holes. We provide a cartoon to help understand the situations in Figure 11.

## 4 Conclusion and Discussion

In this note, we contemplate a physical realization of the black hole chemistry. We use the 8-dimensional Einstein-Yang-Mills-Maxwell system.  $\mathbb{S}^4$ ,  $\mathbb{CP}^2$ , and  $\mathbb{S}^2 \times \mathbb{S}^2$  are regarded as extra dimensions, and a Yang-Mills instanton sits on these four-manifold. Thus, the resultant system becomes an effective 4-dimensional system in the Einstein frame. We only consider phase structures for the asymptotically AdS spacetime since the black hole chemistry has been studied well in the AdS spacetime.

The thermodynamic pressure  $P_{\text{th}}$  is a function of the extra-dimension size  $\mathcal{X}_s$ . In addition, the thermodynamic volume  $V_{\text{th}}$  is determined by a length scale of the black hole horizon. Therefore, one may regard the extra-dimension and the black hole sizes as a thermodynamically conjugate pair in the black hole chemistry.

First, we consider the 4-dimensional Schwarzschild black hole and discuss the well-known Hawking-Page transition. We find phase diagrams in terms of  $\mathcal{X}_s$ ; the results are shown in Figure 3. Also, the restriction to the black hole sizes regarding  $\mathcal{X}_s$  is depicted in Figure 4. From these results, one can notice that the Hawking-Page transition or black hole merging may happen as the extra-dimension size grows. The left cartoon of Figure 11 explains these scenarios.

On the other hand, the dyonic or Kerr-AdS black hole undergoes the Large/Small phase transition as the extra-dimension size or temperature varies in particular ensembles<sup>6</sup>. These two cases have qualitatively similar phase diagrams (Figure 6) and disal-

---

<sup>6</sup>This phase transition is based on the system with fixed charge and external field for the dyonic black hole, and the rotating hole case is based on the canonical ensemble with a fixed angular momentum.

lowed size distributions (Figure 7 and 10), except for the zeroth-order phase transition. From the 4-dimensional perspective, quite large or very small black holes can exist. The intermediate-sized black holes are thermodynamically unstable. Therefore, these black holes should merge with the nearest black holes or absorb close matters to become larger ones. Otherwise, the black holes fission into smaller black holes. We describe this scenario in the right cartoon of Figure 11.

This thermodynamic instability can also be understood as that of objects in the 8-dimensional system. These black holes are black 4-branes with an extra-dimension size. Since the transition is associated with the size of the branes, this thermodynamic property is reminiscent of the Gregory-Laflamme (GL) instability [57]. Relating our result or the black hole chemistry to the GL instability would be interesting. However, the physical situations of GL instability and our thermodynamics, including extra dimensions, are not identical. So, we will leave further study or discussion as one of our future works.

As shown in Figure 6, the black hole chemistry of the Kerr-AdS black hole shows a zeroth-order phase transition in the canonical ensemble. This phenomenon occurs in the high-spinning parameter region. The zeroth-order phase transition is theoretically expected in various cases, as discussed in the introduction. We restrict our solution ansatz with a constant warping factor  $\mathcal{X} = e^{2f}$ . So, it would be desirable to clarify what the instability, with a more general configuration, implies. This is another main issue we need to solve in the future.

As another future study, one may investigate the hairy configuration with a non-trivial warping factor,  $e^{2f(x)}$ . This describes the inhomogeneous extra dimension size of spacetimes. Also, our model can be extended to a 10-dimensional system or with higher derivative terms. The former may allow us to construct a similar system in string theory, and the latter may include a quantum gravity effect on the black hole chemistry. In addition, one may study thermodynamic properties for the de Sitter case, which needs a cavity to find a physically meaningful circumstance. See [27–29] for related works. Such an extension may be a phenomenological application of the black hole chemistry based on the size distribution of existing black holes.

## Acknowledgement

We thank Yunseok Seo and Sang-A Park for their helpful discussions. K. K. Kim thanks Nobuyoshi Ohta for a helpful comment on the magnetic black hole. This work is supported by the Basic Science Research Program through NRF grant No. NRF-2019R1A2C 1007396 (K. K. Kim). We thank members of Korea Research Network for Theoretical Physics for helpful discussions. We acknowledge the hospitality at APCTP, where part of this work was done.

## A D=4 Euclidean Kerr-AdS Black Hole

We briefly summarized the thermodynamics of the Euclidean Kerr-AdS black hole in four dimensions. The analytic continuation of the time coordinate and the rotation parameter is

given by  $t = i\tau$  and  $a = i\hat{a}$  between the Euclidean and Lorentzian systems. The Euclidean metric is

$$ds^2 = \frac{\hat{\rho}^2}{\hat{\Delta}_r} dr^2 + \frac{\hat{\Delta}_r \hat{\rho}^2}{(r^2 - \hat{a}^2)^2} \omega^2 + \frac{\hat{\rho}^2}{\hat{\Delta}_\theta} (d\theta^2 + \sin^2 \theta \tilde{\omega}^2) \quad (\text{A.1})$$

where

$$\hat{\rho}^2 = r^2 - \hat{a}^2 \cos^2 \theta, \quad \hat{\Delta}_r = (r^2 - \hat{a}^2) \left(1 - \frac{V}{6} r^2\right) - 2\mathbf{G}_4 m r \quad (\text{A.2})$$

$$\hat{\Delta}_\theta = 1 - \frac{V}{6} \hat{a}^2 \cos^2 \theta, \quad \hat{\Xi} = 1 - \frac{V}{6} \hat{a}^2, \quad (\text{A.3})$$

$$\omega = \frac{r^2 - \hat{a}^2}{\hat{\rho}^2} \left( d\tau - \frac{\hat{a} \sin^2 \theta}{\hat{\Xi}} d\phi \right), \quad \tilde{\omega} = \hat{\Delta}_\theta \frac{r^2 - \hat{a}^2}{\hat{\Xi} \hat{\rho}^2} \left( d\phi + \frac{\hat{a} \hat{\Xi}}{r^2 - \hat{a}^2} d\tau \right). \quad (\text{A.4})$$

Now, we consider the near horizon geometry by introducing the following coordinate:

$$\hat{\Delta}_r \sim (r - r_+) \hat{\Delta}'_r(r_+) = \frac{\alpha}{4} \eta^2, \quad (\text{A.5})$$

where  $\alpha = \hat{\Delta}'_r(r_+)$ . Then, the metric near horizon is given by

$$\begin{aligned} ds^2 &\sim \frac{\hat{\rho}_+^2}{\alpha} d\eta^2 + \frac{\alpha \eta^2 \hat{\rho}_+^2}{4(r_+^2 - \hat{a}^2)^2} \omega_+^2 + \frac{\hat{\rho}_+^2}{\hat{\Delta}_\theta} (d\theta^2 + \sin^2 \theta \tilde{\omega}_+^2) \\ &= ds_{1\text{st}}^2 + ds_{2\text{nd}}^2, \end{aligned} \quad (\text{A.6})$$

where

$$\omega_+ = \frac{r_+^2 - \hat{a}^2}{\hat{\rho}_+^2} \left( d\tau - \frac{\hat{a} \sin^2 \theta}{\hat{\Xi}} d\phi \right) \quad \text{and} \quad \tilde{\omega}_+ = \hat{\Delta}_\theta \frac{r_+^2 - \hat{a}^2}{\hat{\Xi} \hat{\rho}_+^2} \left( d\phi + \frac{\hat{a} \hat{\Xi}}{r_+^2 - \hat{a}^2} d\tau \right) \quad (\text{A.7})$$

with

$$\hat{\rho}_+^2 = r_+^2 - \hat{a}^2 \cos^2 \theta. \quad (\text{A.8})$$

The second part of the metric is

$$ds_{2\text{nd}}^2 = \frac{\hat{\rho}_+^2}{\hat{\Delta}_\theta} d\theta^2 + \frac{\hat{\rho}_+^2}{\hat{\Delta}_\theta} \left( \hat{\Delta}_\theta \frac{r_+^2 - \hat{a}^2}{\hat{\Xi} \hat{\rho}_+^2} \right)^2 \sin^2 \theta d\psi^2, \quad (\text{A.9})$$

where we introduce an angle coordinate  $\psi = \phi + \frac{\hat{a} \hat{\Xi}}{r_+^2 - \hat{a}^2} \tau$ . The regularity can be justified by the regularity at  $\theta = 0$  and  $\theta = \pi$ . The metric near these points is

$$ds_{2\text{nd}}^2 \sim \frac{r_+^2 - \hat{a}^2}{1 - \frac{V}{6} \hat{a}^2} (d\theta^2 + \sin^2 \theta d\psi^2). \quad (\text{A.10})$$

Therefore, the regularity requires the identification of  $\psi = 0$  and  $\psi = 2\pi$ .

Now, let us focus on the first part at a point  $\theta$  and  $\psi$ . At this point  $d\phi = -\frac{\hat{a} \hat{\Xi}}{r_+^2 - \hat{a}^2} d\tau$ . The  $\omega_+$  becomes

$$\omega_+ = \frac{r_+^2 - \hat{a}^2}{\hat{\rho}_+^2} \left( 1 + \frac{\hat{a}^2 \sin^2 \theta}{r_+^2 - \hat{a}^2} \right) d\tau = d\tau. \quad (\text{A.11})$$

Using this, the first part of the metric

$$ds_{\text{1st}}^2 = \frac{\hat{\rho}_+^2}{\alpha} d\eta^2 + \frac{\alpha\eta^2\hat{\rho}_+^2}{4(r_+^2 - \hat{a}^2)^2} \omega_+^2 = \frac{\hat{\rho}_+^2}{\alpha} \left( d\eta^2 + \frac{\eta^2\alpha^2}{4(r_+^2 - \hat{a}^2)^2} d\tau^2 \right). \quad (\text{A.12})$$

To avoid a conical singularity, the period of  $\tau$  equivalent to the inverse temperature is identified by

$$T = \frac{\hat{\Delta}'_r(r_+)}{4\pi(r_+^2 - \hat{a}^2)}. \quad (\text{A.13})$$

Also,  $\phi$  has a period  $\Omega'/T$  for the regular behavior, where  $\Omega' = \frac{\hat{a}\hat{\Xi}}{r_+^2 - \hat{a}^2}$ . The explicit expression of the temperature is

$$T = \frac{r_+}{4\pi(r_+^2 - \hat{a}^2)} \left( 1 + \frac{\hat{a}^2}{r_+^2} - \frac{1}{2}V \left( r_+^2 - \frac{\hat{a}^2}{3} \right) \right). \quad (\text{A.14})$$

The corresponding expression in the Lorentzian signature is obtained by  $\hat{a} \rightarrow -ia$ . In addition, the conjugate variable entropy is

$$S = \frac{1}{4\mathbf{G}_4} \int_0^{2\pi} d\phi \int_0^\pi d\theta \sqrt{g_{\theta\theta}g_{\phi\phi}} = \frac{\pi}{\mathbf{G}_4} \left( \frac{r_+^2 + a^2}{1 + \frac{V}{6}a^2} \right). \quad (\text{A.15})$$

The Lorentzian angular velocity by the analytic continuation with the time coordinate is

$$\Omega' = \frac{a\Xi}{r_+^2 - a^2}. \quad (\text{A.16})$$

This is identified with the angular velocity, measured relative to a frame rotating at infinity. Therefore, the angular velocity is given by

$$\Omega = \Omega' - \frac{\tilde{\Lambda}_{\text{eff}}}{3}a. \quad (\text{A.17})$$

## References

- [1] D. Kastor, S. Ray and J. Traschen, ‘‘Enthalpy and the Mechanics of AdS Black Holes,’’ *Class. Quant. Grav.* **26**, 195011 (2009) [arXiv:0904.2765 [hep-th]].
- [2] B. P. Dolan, ‘‘The cosmological constant and the black hole equation of state,’’ *Class. Quant. Grav.* **28**, 125020 (2011) [arXiv:1008.5023 [gr-qc]].
- [3] B. P. Dolan, ‘‘Pressure and volume in the first law of black hole thermodynamics,’’ *Class. Quant. Grav.* **28**, 235017 (2011) [arXiv:1106.6260 [gr-qc]].
- [4] M. Cvetič, G. W. Gibbons, D. Kubiznak and C. N. Pope, ‘‘Black Hole Enthalpy and an Entropy Inequality for the Thermodynamic Volume,’’ *Phys. Rev. D* **84**, 024037 (2011) [arXiv:1012.2888 [hep-th]].
- [5] D. Kubiznak and R. B. Mann, ‘‘P-V criticality of charged AdS black holes,’’ *JHEP* **07**, 033 (2012) [arXiv:1205.0559 [hep-th]].

- [6] D. Kubiznak, R. B. Mann and M. Teo, “Black hole chemistry: thermodynamics with Lambda,” *Class. Quant. Grav.* **34**, no.6, 063001 (2017) [arXiv:1608.06147 [hep-th]].
- [7] S. W. Hawking and D. N. Page, “Thermodynamics of Black Holes in anti-De Sitter Space,” *Commun. Math. Phys.* **87**, 577 (1983)
- [8] D. Kubiznak and R. B. Mann, “Black hole chemistry,” *Can. J. Phys.* **93**, no.9, 999-1002 (2015) [arXiv:1404.2126 [gr-qc]].
- [9] E. Witten, “Anti-de Sitter space, thermal phase transition, and confinement in gauge theories,” *Adv. Theor. Math. Phys.* **2**, 505-532 (1998) [arXiv:hep-th/9803131 [hep-th]].
- [10] M. Henneaux and C. Teitelboim, “THE COSMOLOGICAL CONSTANT AS A CANONICAL VARIABLE,” *Phys. Lett. B* **143**, 415-420 (1984)
- [11] C. Teitelboim, “THE COSMOLOGICAL CONSTANT AS A THERMODYNAMIC BLACK HOLE PARAMETER,” *Phys. Lett. B* **158**, 293-297 (1985)
- [12] J. D. E. Creighton and R. B. Mann, “Quasilocal thermodynamics of dilaton gravity coupled to gauge fields,” *Phys. Rev. D* **52**, 4569-4587 (1995) [arXiv:gr-qc/9505007 [gr-qc]].
- [13] N. Altamirano, D. Kubiznak and R. B. Mann, “Reentrant phase transitions in rotating anti-de Sitter black holes,” *Phys. Rev. D* **88**, no.10, 101502 (2013) [arXiv:1306.5756 [hep-th]].
- [14] A. M. Frassino, D. Kubiznak, R. B. Mann and F. Simovic, “Multiple Reentrant Phase Transitions and Triple Points in Lovelock Thermodynamics,” *JHEP* **09**, 080 (2014) [arXiv:1406.7015 [hep-th]].
- [15] N. Altamirano, D. Kubizňák, R. B. Mann and Z. Sherkatghanad, “Kerr-AdS analogue of triple point and solid/liquid/gas phase transition,” *Class. Quant. Grav.* **31**, 042001 (2014) [arXiv:1308.2672 [hep-th]].
- [16] S. W. Wei and Y. X. Liu, “Triple points and phase diagrams in the extended phase space of charged Gauss-Bonnet black holes in AdS space,” *Phys. Rev. D* **90**, no.4, 044057 (2014) [arXiv:1402.2837 [hep-th]].
- [17] A. Dehghani, S. H. Hendi and R. B. Mann, “Range of novel black hole phase transitions via massive gravity: Triple points and  $N$ -fold reentrant phase transitions,” *Phys. Rev. D* **101**, no.8, 084026 (2020) [arXiv:2009.07980 [hep-th]].
- [18] N. Altamirano, D. Kubiznak, R. B. Mann and Z. Sherkatghanad, “Thermodynamics of rotating black holes and black rings: phase transitions and thermodynamic volume,” *Galaxies* **2**, 89-159 (2014) [arXiv:1401.2586 [hep-th]].
- [19] C. V. Johnson, “Holographic Heat Engines,” *Class. Quant. Grav.* **31**, 205002 (2014) [arXiv:1404.5982 [hep-th]].
- [20] B. P. Dolan, A. Kostouki, D. Kubiznak and R. B. Mann, “Isolated critical point from Lovelock gravity,” *Class. Quant. Grav.* **31**, no.24, 242001 (2014) [arXiv:1407.4783 [hep-th]].
- [21] R. A. Hennigar, R. B. Mann and E. Tjoa, “Superfluid Black Holes,” *Phys. Rev. Lett.* **118**, no.2, 021301 (2017) [arXiv:1609.02564 [hep-th]].
- [22] S. W. Wei and Y. X. Liu, “Insight into the Microscopic Structure of an AdS Black Hole from a Thermodynamical Phase Transition,” *Phys. Rev. Lett.* **115**, no.11, 111302 (2015) [erratum: *Phys. Rev. Lett.* **116**, no.16, 169903 (2016)] [arXiv:1502.00386 [gr-qc]].
- [23] M. Astorino, “Thermodynamics of Regular Accelerating Black Holes,” *Phys. Rev. D* **95**, no.6, 064007 (2017) [arXiv:1612.04387 [gr-qc]].

- [24] A. Anabalón, M. Appels, R. Gregory, D. Kubizňák, R. B. Mann and A. Ovgün, “Holographic Thermodynamics of Accelerating Black Holes,” *Phys. Rev. D* **98**, no.10, 104038 (2018) [arXiv:1805.02687 [hep-th]].
- [25] A. Anabalón, F. Gray, R. Gregory, D. Kubizňák and R. B. Mann, “Thermodynamics of Charged, Rotating, and Accelerating Black Holes,” *JHEP* **04**, 096 (2019) [arXiv:1811.04936 [hep-th]].
- [26] J. Wu and R. B. Mann, “Thermodynamically stable phases of asymptotically flat Lovelock black holes,” *Class. Quant. Grav.* **40**, no.14, 145009 (2023) [arXiv:2212.08673 [hep-th]].
- [27] B. P. Dolan, D. Kastor, D. Kubiznak, R. B. Mann and J. Traschen, “Thermodynamic Volumes and Isoperimetric Inequalities for de Sitter Black Holes,” *Phys. Rev. D* **87**, no.10, 104017 (2013) [arXiv:1301.5926 [hep-th]].
- [28] S. Mbarek and R. B. Mann, “Reverse Hawking-Page Phase Transition in de Sitter Black Holes,” *JHEP* **02**, 103 (2019) [arXiv:1808.03349 [hep-th]].
- [29] F. Simovic and R. B. Mann, “Critical Phenomena of Charged de Sitter Black Holes in Cavities,” *Class. Quant. Grav.* **36**, no.1, 014002 (2019) [arXiv:1807.11875 [gr-qc]].
- [30] S. Mbarek and R. B. Mann, “Thermodynamic Volume of Cosmological Solitons,” *Phys. Lett. B* **765**, 352-358 (2017) [arXiv:1611.01131 [hep-th]].
- [31] C. Quijada, A. Anabalón, R. B. Mann and J. Oliva, “Triple points of gravitational AdS solitons and black holes,” *Phys. Rev. D* **110**, no.2, L021902 (2024) [arXiv:2308.16341 [hep-th]].
- [32] J. M. Maldacena, “The Large N limit of superconformal field theories and supergravity,” *Adv. Theor. Math. Phys.* **2**, 231-252 (1998) [arXiv:hep-th/9711200 [hep-th]].
- [33] A. Karch and B. Robinson, “Holographic Black Hole Chemistry,” *JHEP* **12**, 073 (2015) [arXiv:1510.02472 [hep-th]].
- [34] M. Sinamuli and R. B. Mann, “Higher Order Corrections to Holographic Black Hole Chemistry,” *Phys. Rev. D* **96**, no.8, 086008 (2017) [arXiv:1706.04259 [hep-th]].
- [35] W. Cong, D. Kubiznak and R. B. Mann, “Thermodynamics of AdS Black Holes: Critical Behavior of the Central Charge,” *Phys. Rev. Lett.* **127**, no.9, 091301 (2021) [arXiv:2105.02223 [hep-th]].
- [36] K. K. Kim and B. Ahn, “Thermodynamic Volume in AdS/CFT,” *EPJ Web Conf.* **168**, 07003 (2018)
- [37] M. B. Ahmed, W. Cong, D. Kubizňák, R. B. Mann and M. R. Visser, “Holographic Dual of Extended Black Hole Thermodynamics,” *Phys. Rev. Lett.* **130**, no.18, 181401 (2023) [arXiv:2302.08163 [hep-th]].
- [38] R. B. Mann, “Recent Developments in Holographic Black Hole Chemistry,” *JHAP* **4**, no.1, 1-26 (2024) [arXiv:2403.02864 [hep-th]].
- [39] S. Randjbar-Daemi, A. Salam and J. A. Strathdee, “Stability of Instanton Induced Compactification in Eight-dimensions,” *Nucl. Phys. B* **242**, 447-472 (1984)
- [40] K. K. Kim, S. Koh and H. S. Yang, “Expanding Universe and Dynamical Compactification Using Yang-Mills Instantons,” *JHEP* **12**, 085 (2018) [arXiv:1810.12291 [hep-th]].
- [41] K. K. Kim, S. Koh and G. Tumurtushaa, “Dynamical Compactification with Matter,” *JHEP* **06**, 181 (2023) [arXiv:2303.13758 [hep-th]].

- [42] J. Ho, K. K. Kim, S. Koh and H. S. Yang, “Generalization of instanton-induced inflation and dynamical compactification,” *JHEP* **11**, 050 (2023) [arXiv:2309.02056 [hep-th]].
- [43] J. Ho, K. K. Kim and H. S. Yang, “Einstein Structure of Squashed Four-Spheres,” [arXiv:2309.05335 [math.DG]].
- [44] S. Gunasekaran, R. B. Mann and D. Kubiznak, “Extended phase space thermodynamics for charged and rotating black holes and Born-Infeld vacuum polarization,” *JHEP* **11**, 110 (2012) [arXiv:1208.6251 [hep-th]].
- [45] M. B. J. Poshteh, B. Mirza and Z. Sherkatghanad, “Phase transition, critical behavior, and critical exponents of Myers-Perry black holes,” *Phys. Rev. D* **88**, no.2, 024005 (2013) [arXiv:1306.4516 [gr-qc]].
- [46] D. C. Zou, Y. Liu and B. Wang, “Critical behavior of charged Gauss-Bonnet AdS black holes in the grand canonical ensemble,” *Phys. Rev. D* **90**, no.4, 044063 (2014) [arXiv:1404.5194 [hep-th]].
- [47] R. A. Hennigar, W. G. Brenna and R. B. Mann, “P-v criticality in quasitopological gravity,” *JHEP* **07**, 077 (2015) [arXiv:1505.05517 [hep-th]].
- [48] R. A. Hennigar and R. B. Mann, “Reentrant phase transitions and van der Waals behaviour for hairy black holes,” *Entropy* **17**, no.12, 8056-8072 (2015) [arXiv:1509.06798 [hep-th]].
- [49] D. Kubiznak and F. Simovic, “Thermodynamics of horizons: de Sitter black holes and reentrant phase transitions,” *Class. Quant. Grav.* **33**, no.24, 245001 (2016) [arXiv:1507.08630 [hep-th]].
- [50] S. W. Wei, P. Cheng and Y. X. Liu, “Analytical and exact critical phenomena of  $d$ -dimensional singly spinning Kerr-AdS black holes,” *Phys. Rev. D* **93**, no.8, 084015 (2016) [arXiv:1510.00085 [gr-qc]].
- [51] A. Dehyadegari, A. Sheykhi and A. Montakhab, “Novel phase transition in charged dilaton black holes,” *Phys. Rev. D* **96**, no.8, 084012 (2017) [arXiv:1707.05307 [hep-th]].
- [52] M. M. Stetsko, “Slowly rotating Einstein–Maxwell-dilaton black hole and some aspects of its thermodynamics,” *Eur. Phys. J. C* **79**, no.3, 244 (2019) [arXiv:1812.10838 [hep-th]].
- [53] B. P. Dolan, “General SU(2) Classical Instanton Configurations in Curved Space Times,” *J. Phys. A* **14**, 1205 (1981)
- [54] S. Hyun, J. Jeong, S. A. Park and S. H. Yi, “Thermodynamic Volume and the Extended Smarr Relation,” *JHEP* **04**, 048 (2017) [arXiv:1702.06629 [hep-th]].
- [55] N. Arkani-Hamed, L. Motl, A. Nicolis and C. Vafa, “The String landscape, black holes and gravity as the weakest force,” *JHEP* **06**, 060 (2007) [arXiv:hep-th/0601001 [hep-th]].
- [56] S. Kachru, R. Kallosh, A. D. Linde and S. P. Trivedi, “De Sitter vacua in string theory,” *Phys. Rev. D* **68**, 046005 (2003) [arXiv:hep-th/0301240 [hep-th]].
- [57] R. Gregory and R. Laflamme, “Black strings and p-branes are unstable,” *Phys. Rev. Lett.* **70**, 2837-2840 (1993) [arXiv:hep-th/9301052 [hep-th]].